

# Prospective Applications for PwrSoC

## *Magnetics and Packaging Technologies*

IEEE PwrSoC Corridor Webinar

5<sup>th</sup> November 2020

*Séamus O'Driscoll, PI Integrated Power Systems*

*seamus.odriscoll@tyndall.ie*

Revision: vsubmit2





# Introduction

Planar inductors for PwrSiP/PwrSoC POL or SoC iVR.

Resonant transformers for isolated bias, large step ratio POL

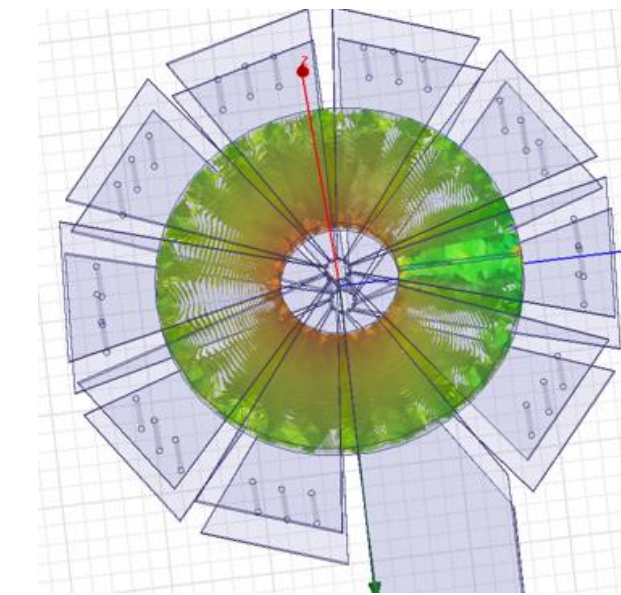
Gate Drivers: Isolated power and signal coupling

ULP Smart Sensor node for IoT

**95+% efficient** magnetic components, at high frequencies, to cater for deep levels of integration

Topologies & Requirements for 4 nH to 1  $\mu$ H magnetising inductance

Systems Perspective:  $L/\text{mm}^2$ ,  $Q_{AC\_LS}$ , DCR,  $\eta_{DEVICE}$ ,  $I_{SAT}$ ,  $C_{CM}$ ,  $C_{IO}$ ,  $\mu_{A\_DCbias}$ , Near field/flux containment



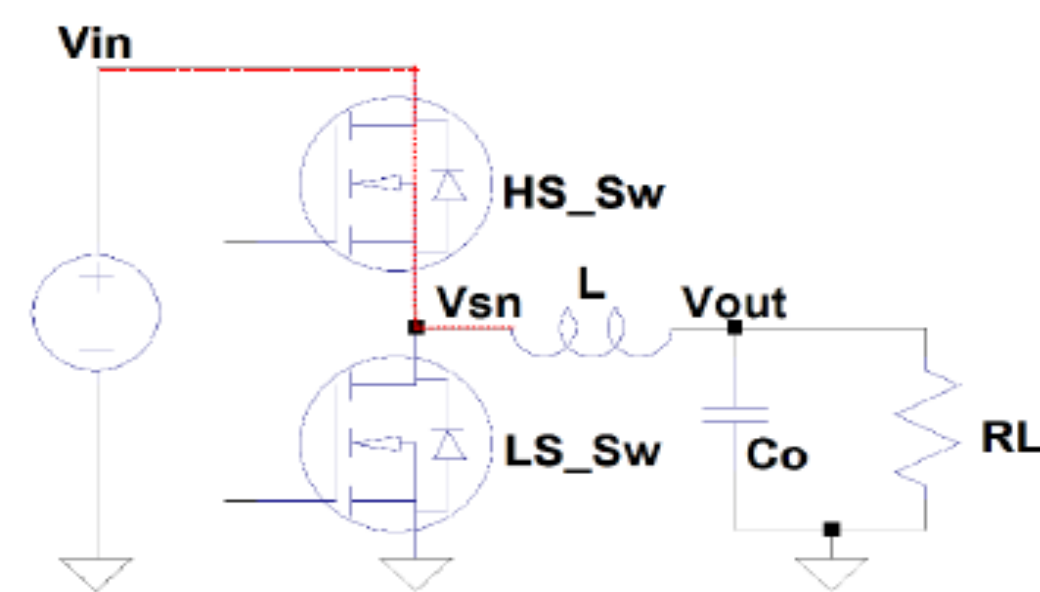
400  $\mu$ m substrate  
embedded toroid



4  $\mu$ m films in planar  
solenoid format (**MoS**)

# Multi-Level Reduces Inductance Value

1. Typical 5 – 1V8 @ 1A POL for portable device is a 3 MHz Buck converter with 1  $\mu$ H inductor; typically a multi-layer ferrite chip; 1008 case size ( 2.5 X 2 X 1 mm).
2. iVR for SoC inductor: a 100 MHz, 1V8 – 1V @ 0.5A requires 4 – 10 nH

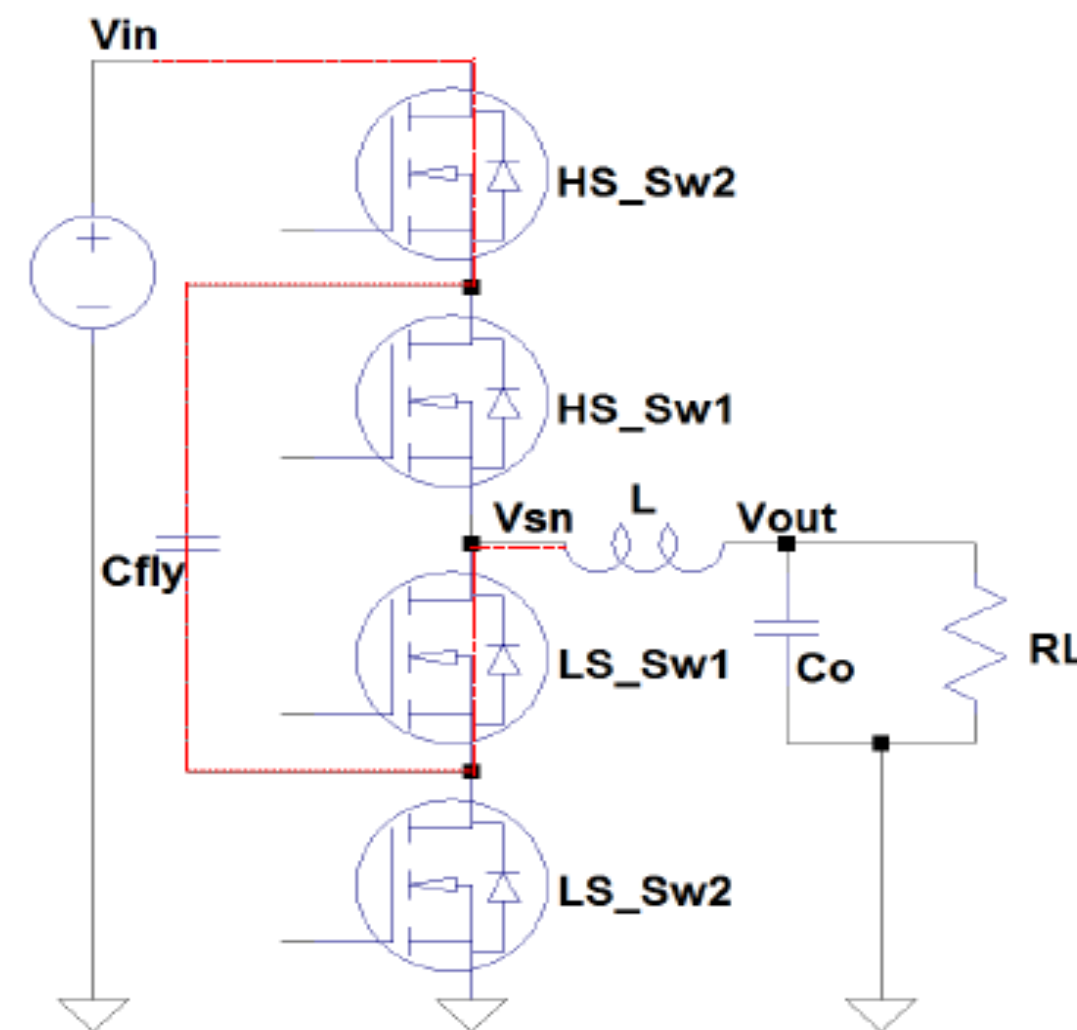
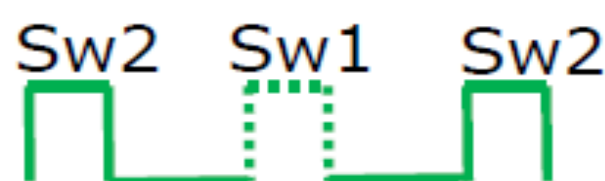


Basic Buck Converter  
(2-L)

Vsn (2-L)



Vsn (3-L)



3-Level Buck Converter

$$C_{fly} = V_{in}/2$$

$$V_L \cdot dt = L \cdot di = N \cdot A_e \cdot dB$$

Multi-Level reduces **volt.seconds**

3-L => 1/2 switch node voltage

3-L => 2 X inductor frequency vs  $f_s$

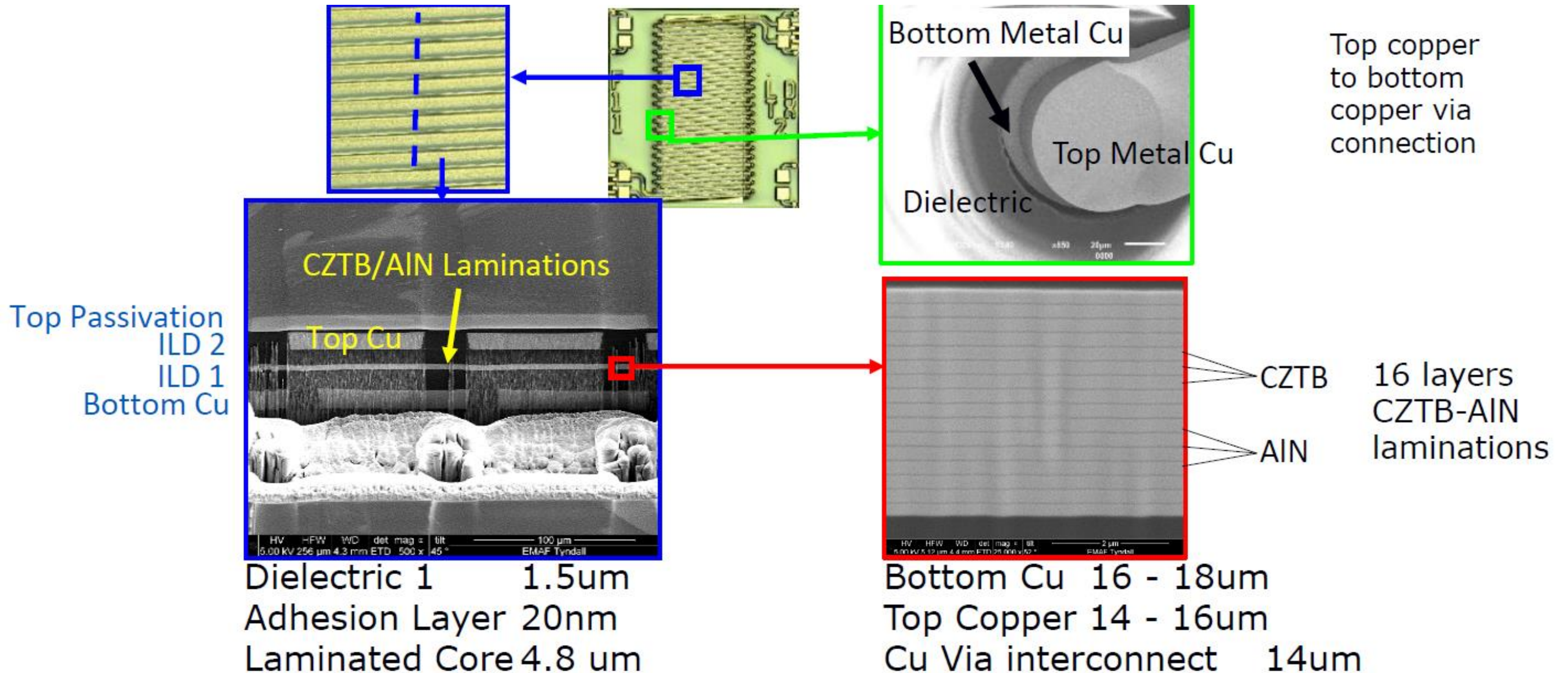
3-L => 2 X Duty Cycle – *possibly very useful for effective coupling!*

4-L => 9 X Reduction in volt-seconds and combine with resonant waveshapes => L value reduction to 10 nH demonstrated for a 5 MHz switcher<sup>1</sup>

*"A 93.8% Peak Efficiency, 5V-Input, 10A Max ILOAD Flying Capacitor Multilevel Converter in 22nm CMOS Featuring Wide Output Voltage Range and Flying Capacitor Precharging", Christopher Schaefer et al., ISSCC 2019, Session 8.1"*



# Solenoid Micro-fabricated Device (SEM, FIB, Photo)

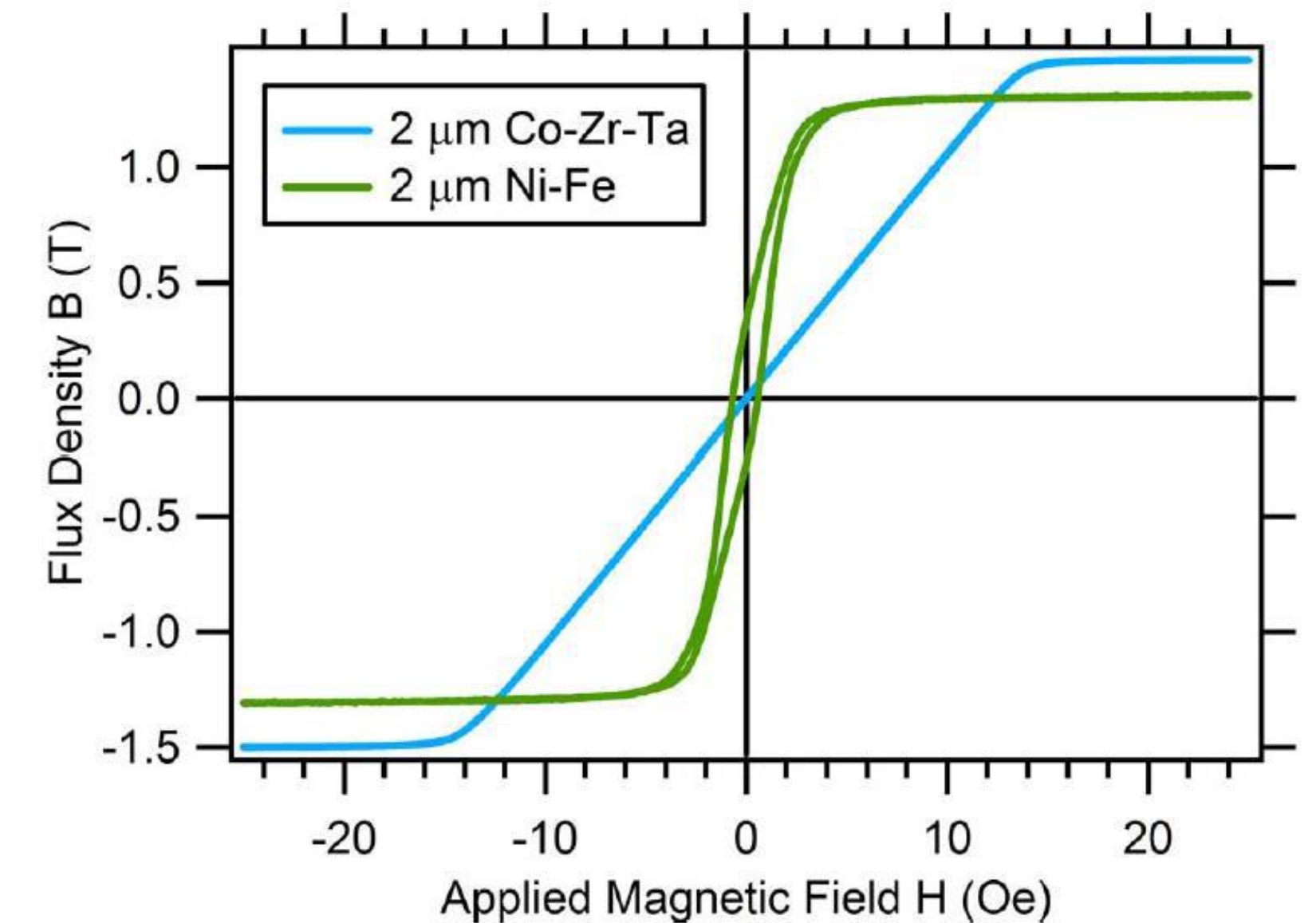


EI "MagPwr" Project CF-2017-0791-P



# Cobalt Based Thin Film Devices, CZT(B)

Symbol [Unit]	No core/ Air-core	Ferrite core	Metallic thin film
$\mu_r$	1	15 – 150 @ 10 MHz+	100 – 700 4 $\mu\text{m}$
$f_{\text{SW}}$ [MHz]	$\infty$	< 12	10 - 200
$B_{\text{sat}}$ [Tesla]	$\infty$	0.1 – 0.2 @ 10 MHz+	1.2 – 1.5 @ 10 MHz+
-	Excellent	Incompatible	Compatible



Donald S. Gardner et al. (INTEL)  
Review of On-Chip Inductor Structures With  
Magnetic Films  
IEEE TRANSACTIONS ON MAGNETICS, VOL.  
45, NO. 10, OCTOBER 2009

- High saturation magnetisation ✓
- Sputtered Cobalt devices achieve adequate  $Q_{\text{LS}}$  for 95+% efficient devices over 10 – 200 MHz; 1 – 5 m $\Omega$ /nH and 10 -50 nH/mm<sup>2</sup> ✓
- Best ferrite power devices really struggle above 10 MHz. CZT good to 100+ MHz ✓
- CZT devices increase L density by 6X (< ~ 10 nH) and 20X (> ~ 100 nH) over air-core ✓



# 2-L 5V @ 30 MHz with 50 nH Inductor

Tyndall fabricated 50nH, 80 mΩ inductor presented at IEEE PwrSoC 2018, [2] P. Podder et al.,

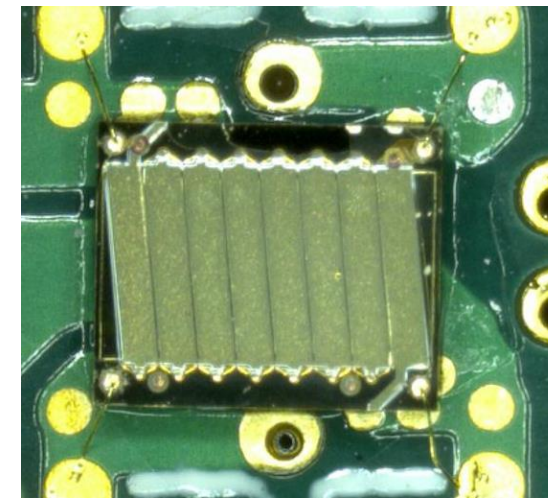
Solenoidal inductors are high Q, because of the “air-gap” portion (excl. adjacent eddy losses). Slightly higher than projected for race-track, [1] Jaime Lopez et al.

Device in 2-L (1-φ) Buck Converter @ 30 MHz

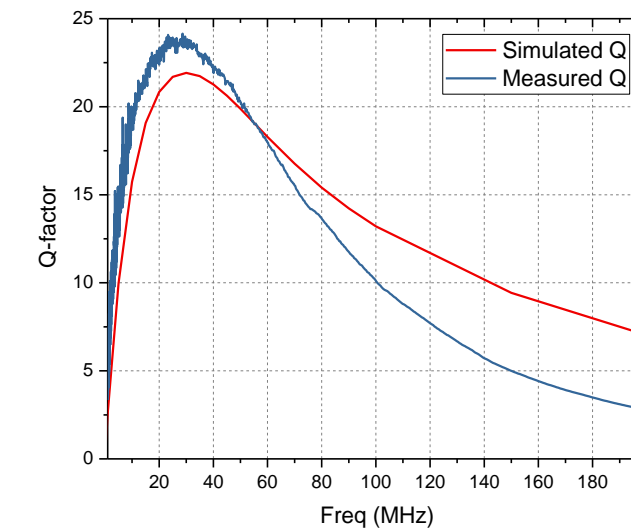
3.45 V to 1.45 V @ 0.5 A = 81 %,

Inductor Loss = 4.31%

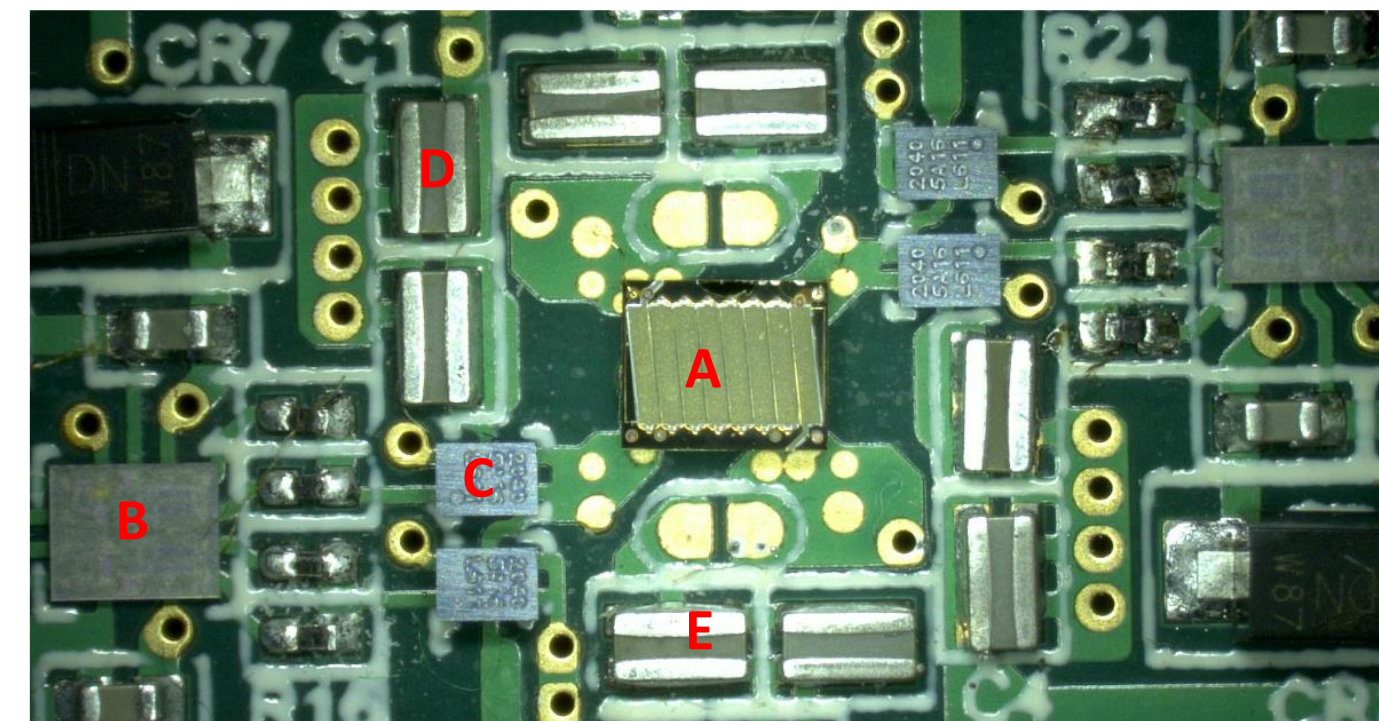
DCR Loss = 3.4%, AC Loss = 0.91%



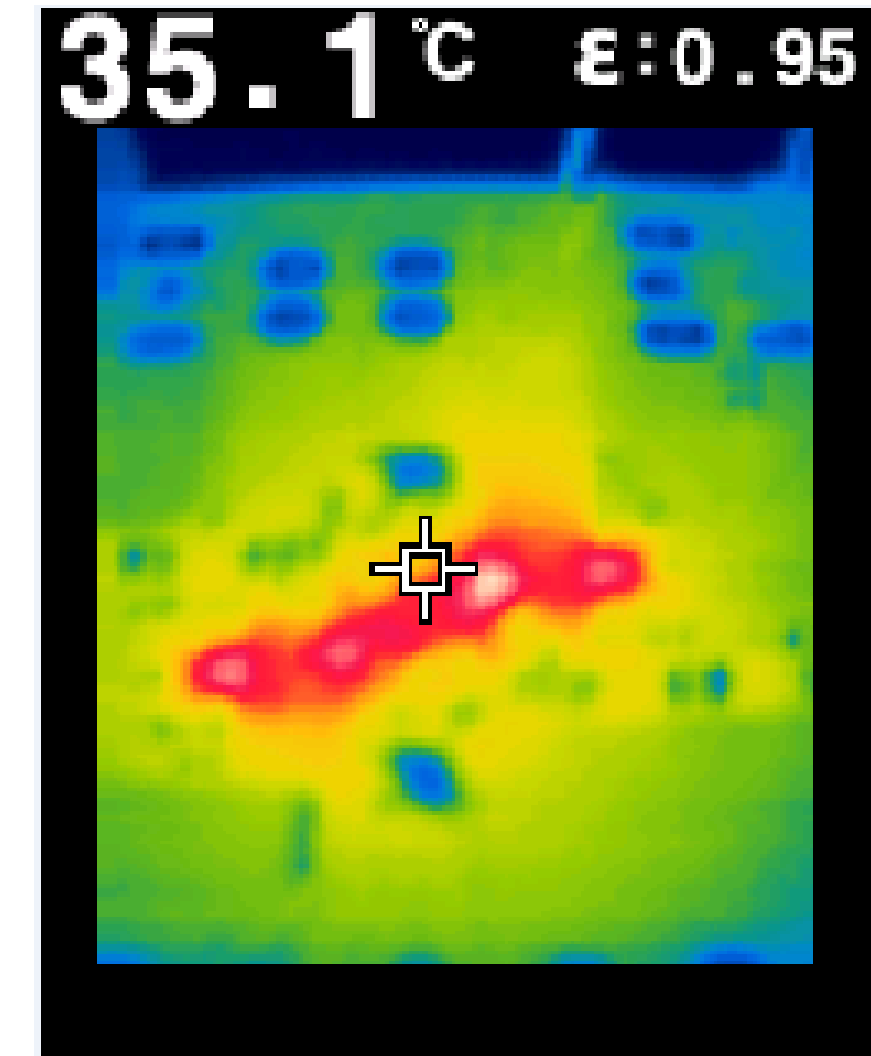
50 nH thin film CZTB  
2 X 1.8mm



$Q_{ss} = 24 @ 30 \text{ MHz}$



Symmetrical 2-Phase Buck Converter  
A. Thin Film CZTB 50 nH on Silicon  
B. Murata-Peregrine-Semi PE29102 Driver  
C. EPC 2040 eHEMT GaN 24mΩ Switches  
D. Input Capacitors (0306 – low ESL)  
E. Output Capacitors (0306 – low ESL)



2-φ Unit: inductor does not show on heat map

L	50nH	B <sub>SAT</sub>	1.2T
DCR	125mΩ	I <sub>SAT</sub>	0.9A
Core Thickness	4 μm	SRF (FMR)	300MHz
Material	CZTB	C <sub>SELF</sub>	3pF(1GHz)
CZTB Lamination	250nm	Cu	15μm
Q <sub>ss_peak</sub>	24		



# Single Inductor Solenoid: Q scaling

**Table 1** Design specifications for single and coupled inductors and transformers

Device type	Device ID	Parameters			
		L [nH]	k12	Footprint [mm <sup>2</sup> ]	$f_{sw}$ [MHz]
Single inductor	SL1	10.4	-	0.5	40
	SL3	105.7	-	2.1	40
	SL4	243.4	-	4.1	40
Coupled inductor	CL2	53.6	0.7	2.6	40
	CL3	104.6	0.8	4.4	40
Transformer	TX1	103.5	0.9	5.1	30
	TX2	40.2	0.9	2.3	30

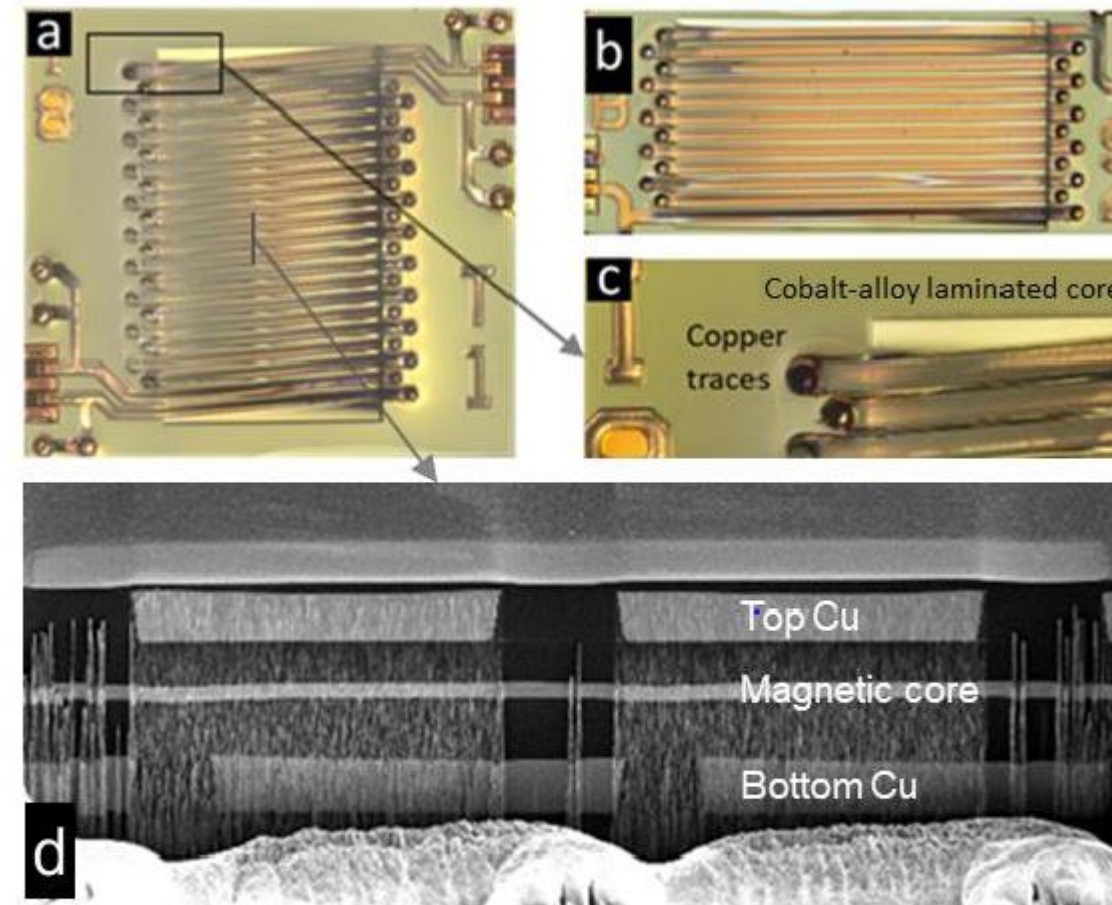
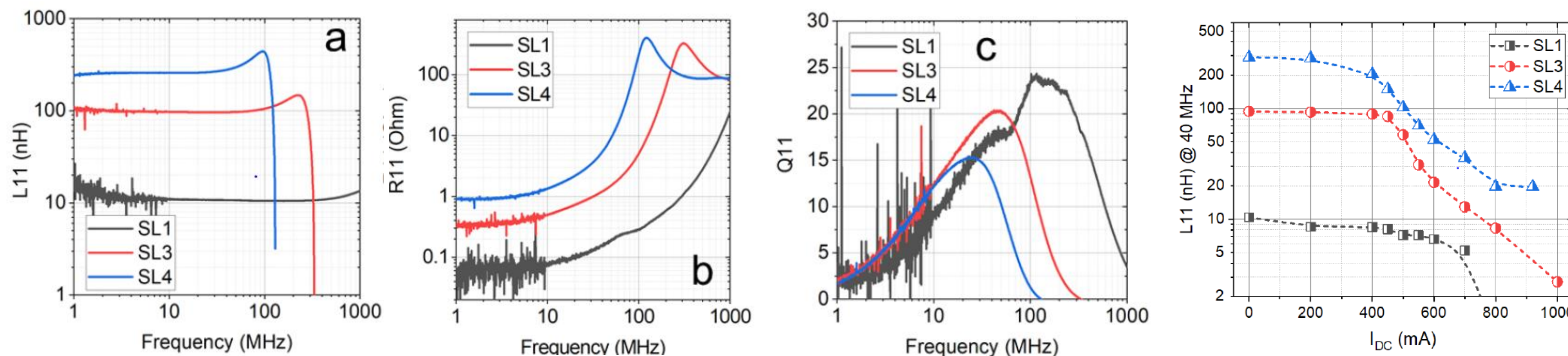


**Figure 2** Fabricated devices a) Transformer, b) Single inductor, c) Enlarged view of cobalt-alloy based laminated core enclosed by copper traces in solenoid construction. d) SEM of the fabricated micro-inductors cross-section.

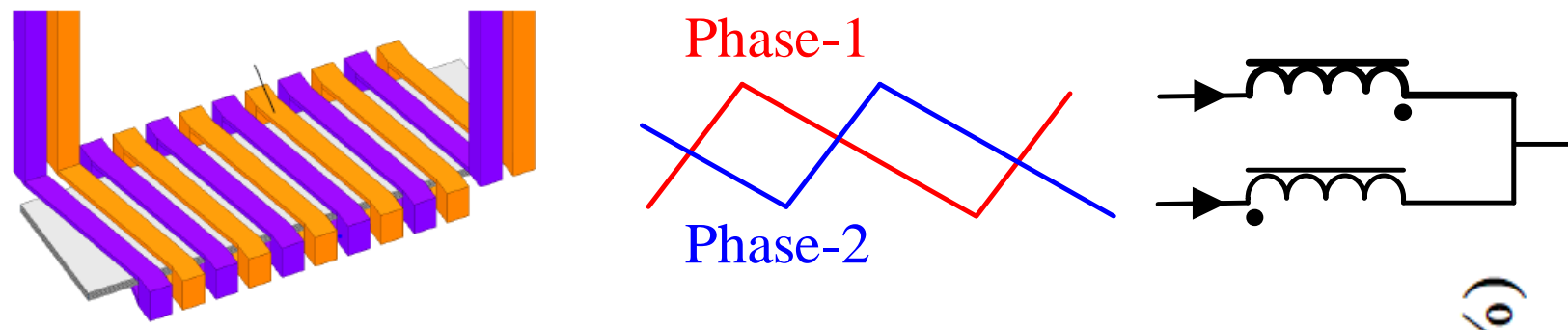
- $f_{-Qpeak}$  scales inversely with N or  $\sqrt{L}$   
- a nice property!
- $L/DCR \sim 0.25 \text{ nH/m}\Omega$   
-  $\sim 1.5\%$  inductor DC loss for Tyndall 100 MHz 4 nH L on 28 nm CMOS



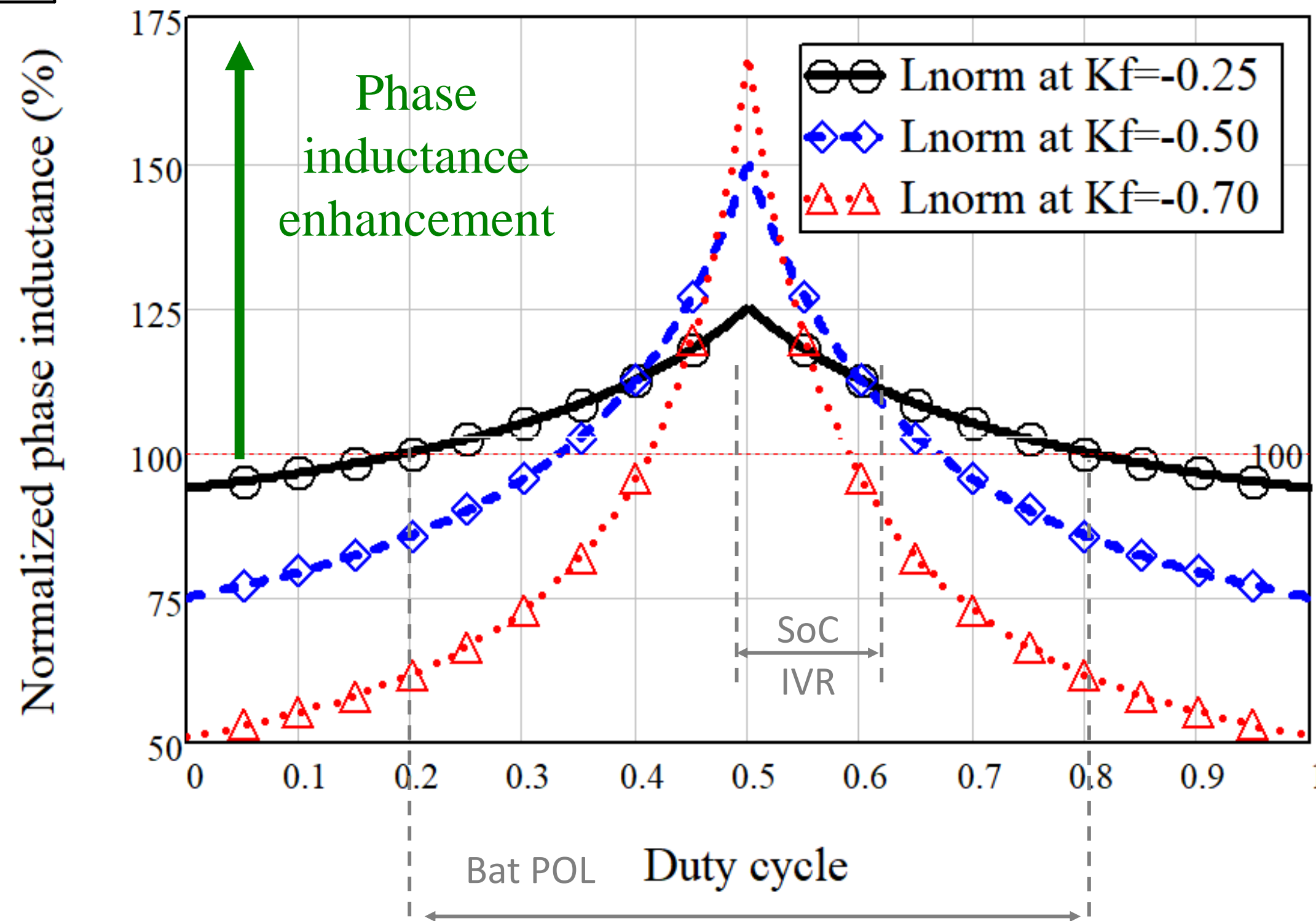
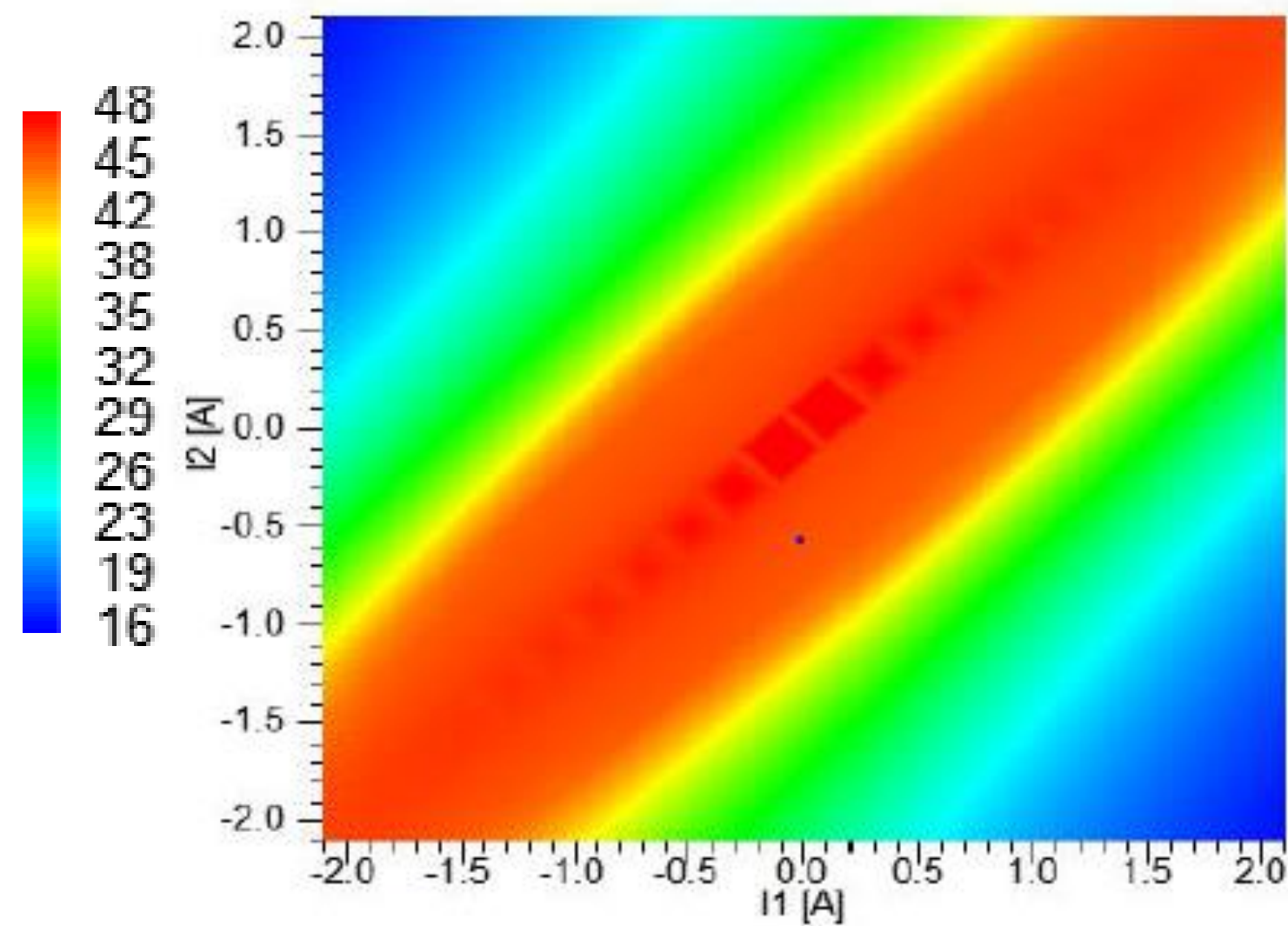
[3] P. Podder et al., Tyndall, Chor Shu Cheng et al., Global Foundries



# 2-Phase Inverse Coupled Inductor

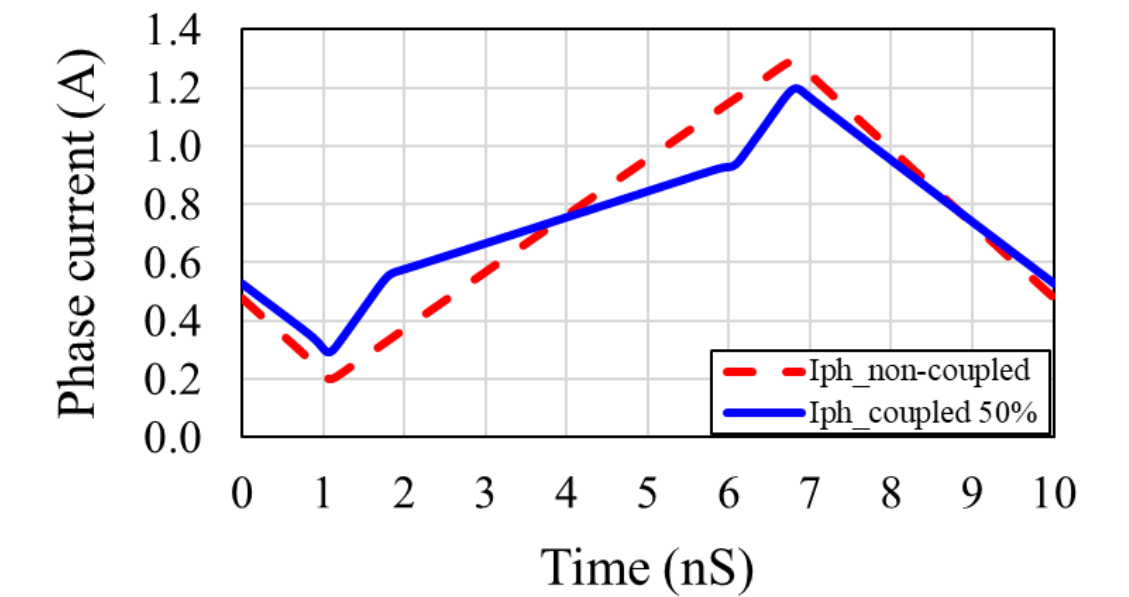


L11 (nH) vs (I1,I2)

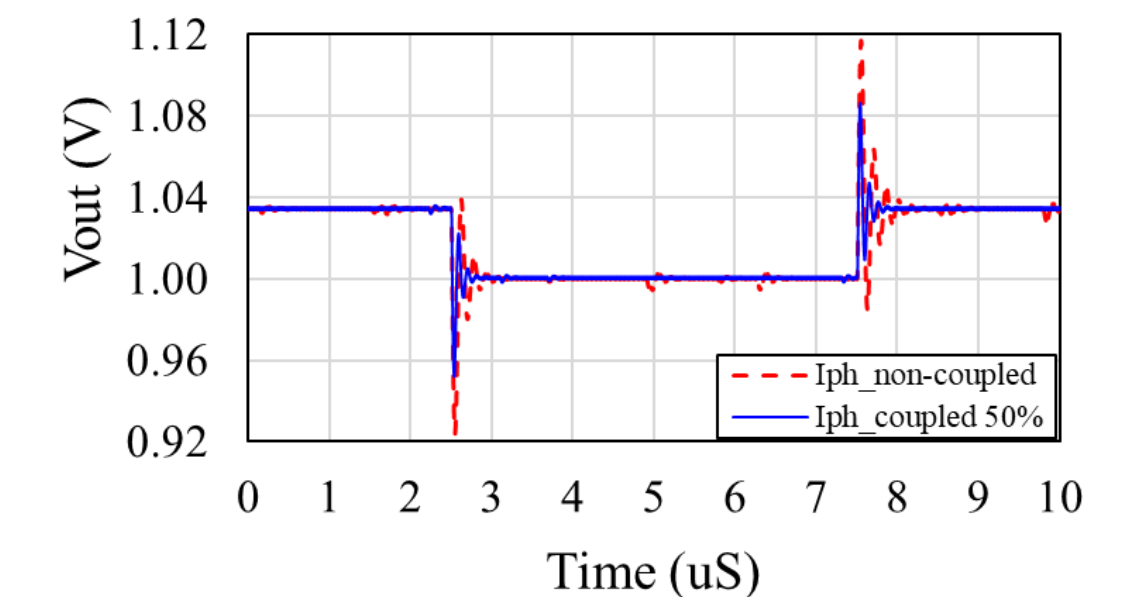


Phase current: 1.8 to 1 V

$$\Delta I_{\text{non-coupled}} = 1.1\text{A}, \Delta I_{\text{Coupled}} = 0.9\text{A}$$



Open loop transient response



- Considering SoC iVR and wide-input-range general purpose battery powered POL
- Reduces DC/ AC fields, size, ripple, increases  $L_{SS}$ , increases  $I_{SAT}$ , improves  $\Delta V_{TR}$

[4] Youssef Kandeel, NUIG, et al., APEC 2019



# Thin Film Solenoids – Other General Observations

$Q_{IS}$  remains flat or increases slightly with increasing DC bias ✓

Generally  $Q_{IS}$  remains high (>13 device Q) up to  $I_{AC\_pk} > 50\% I_{SAT}$  ✓

For some lower inductance devices,  $Q_{IS} > 80\% Q_{SS}$  @  $I_{AC\_pk} = I_{SAT}$

Practical, high-Q, inductor density (L/mm<sup>2</sup>) = **X6** over air-core (tf-solenoid) for ~10 nH and **X25** over air-core for ~ 100 nH ✓



# Thin Film magnetic Layers on PCB

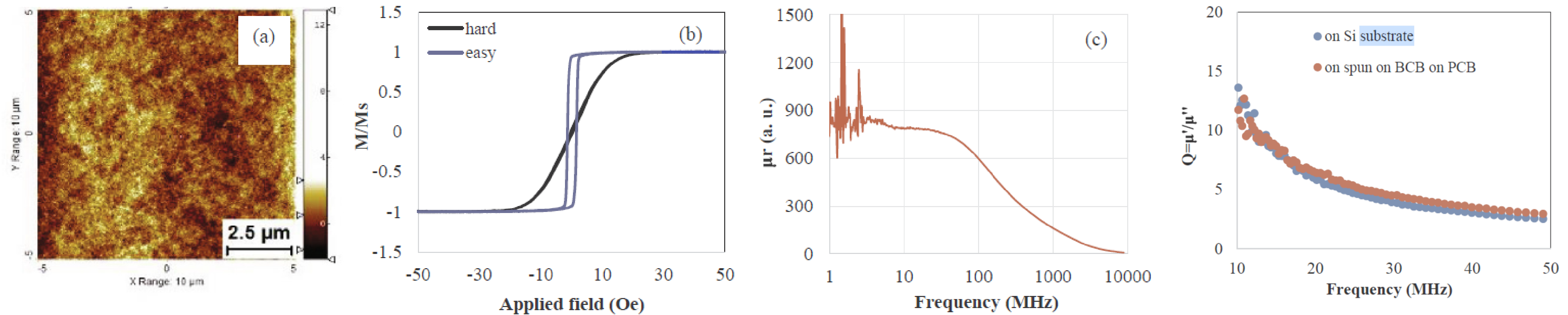


Fig. 6. (a) AFM results for BCB spun onto PCB before any deposition of magnetic material, (b, c) *B-H* loop and high frequency permeability for Ni<sub>45</sub>Fe<sub>55</sub> deposited on BCB spun on to PCB (with O<sub>2</sub> treatment) respectively.

Ni<sub>45</sub>Fe<sub>55</sub> Properties similar to on-silicon if pre-treat. Average roughness, Ra = 23 nm (PCB) vs 0.4 nm (Si)

This enables electroplated or sputtered films to be deposited on PCB with good high frequency properties

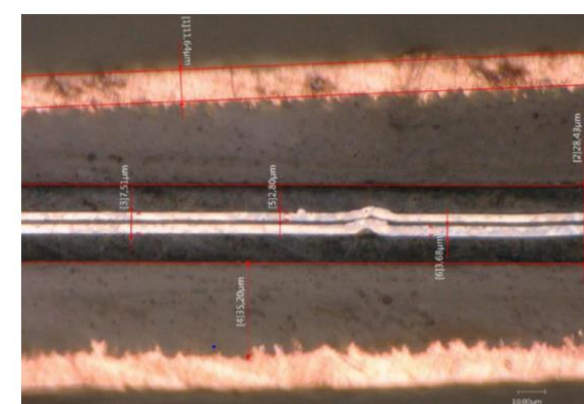
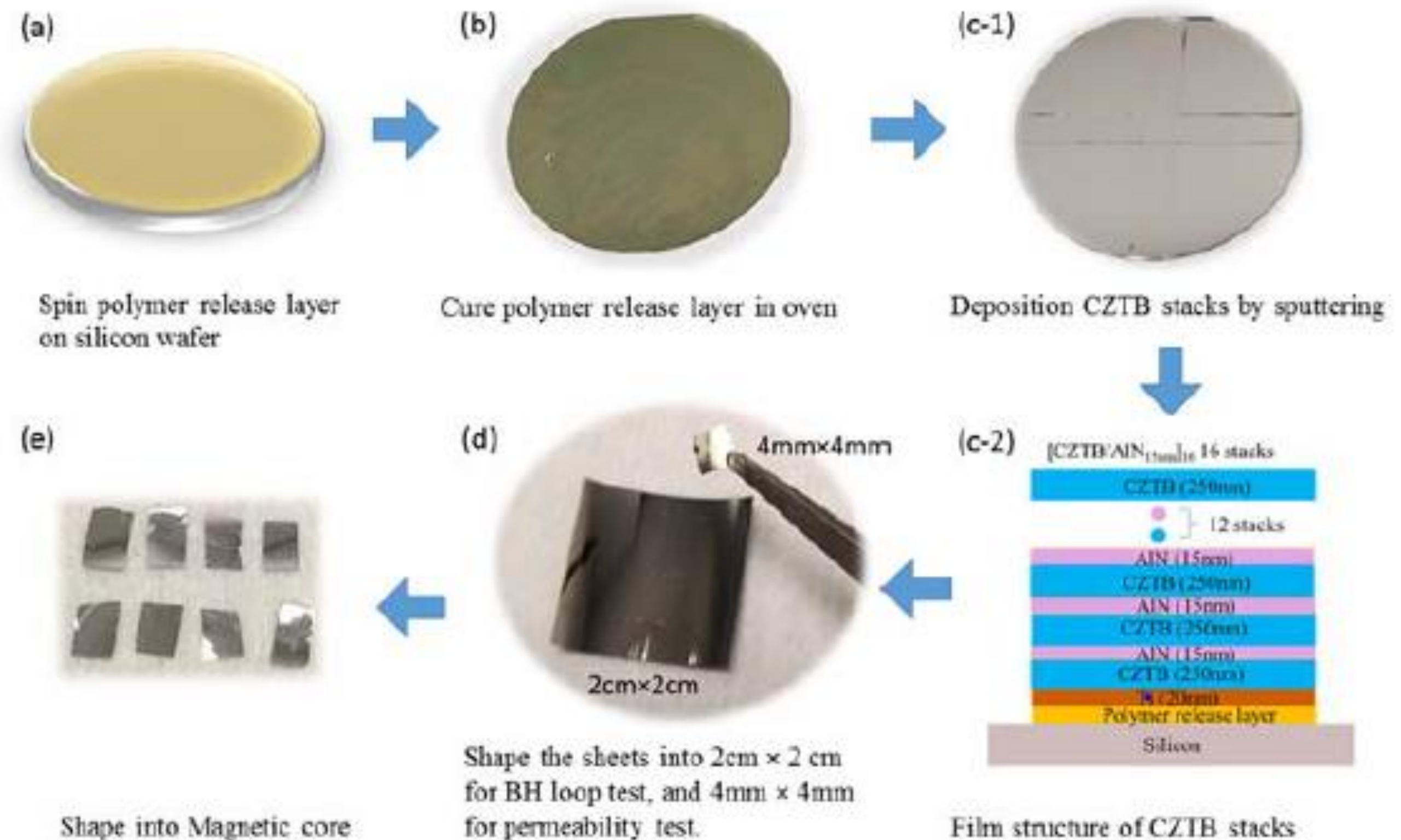
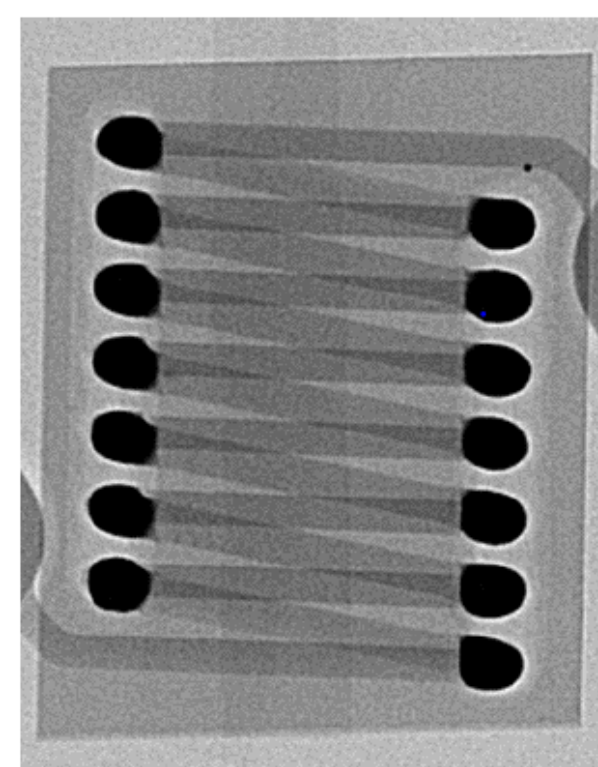
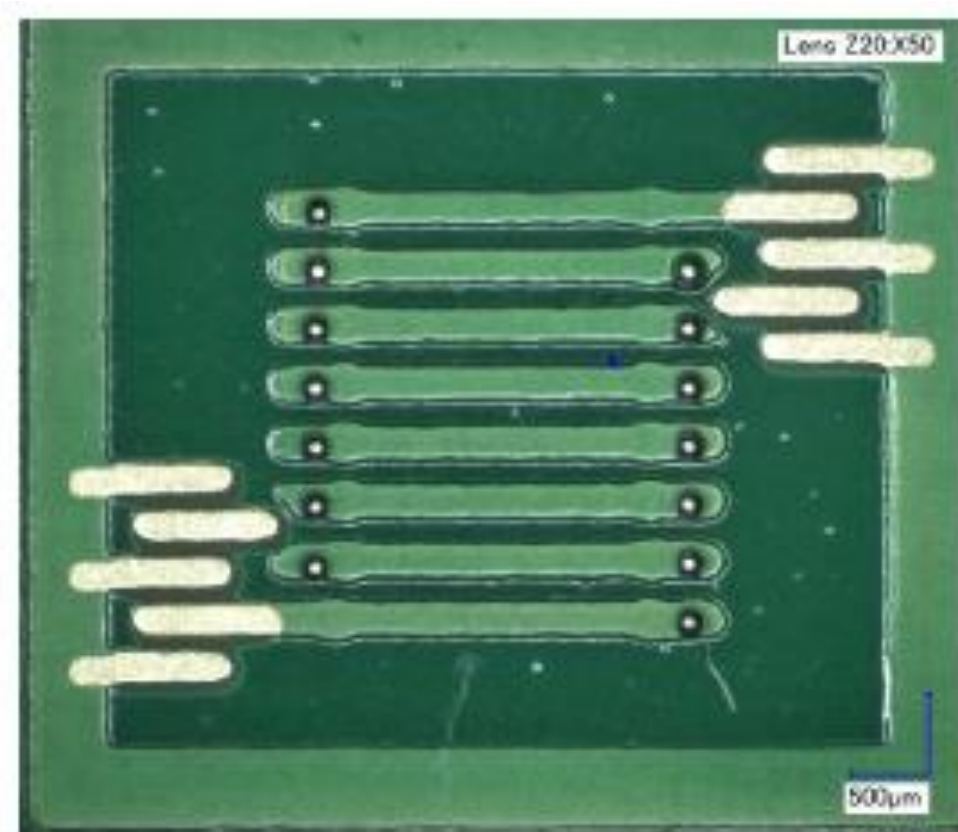
[5] Zhara Ghaferi et al., Tyndall. EU H2020 “GaNonCMOS” [www.ganoncmos.eu](http://www.ganoncmos.eu)





# PwrSiP: Multi-Layer CZTB in Flip Chip PCB

Solenoidal inductor device design  
 Enables 70 – 150 um Cu thickness  
 Retains high Q at 40 MHz (Q= 23)  
 Cost effective Flip Chip approach  
 No via drill holes, Good DCR



Layers	2
Layer Thickness	2 um
Layer Separation	2 um

*Embedded Tyndall laminated film has passed reliability trials in GaNonCMOS program*



[6] Declan Jordan et al. Tyndall 2 X 2.8 mm CZTB film



# Co-sputtering SiO<sub>2</sub> and CZTB

- Increases Q – small signal  $\gg 100$  @ 300 MHz
  - (single layer films have very high  $\mu$  and Q)
- Maintains well-aligned uniaxial magnetic anisotropy
- P CZTB-SiO<sub>2</sub> increases to 224  $\mu\Omega$  cm to allow higher lamination thicknesses (< skin depth)
  - Fewer laminations, lower cost
- Enables an additional control handle over permeability.
  - High frequency power ferrites achieve low loss by reducing  $\mu_r$  to 15-50 range.
  - Potential advantage for closed-core (race-track)

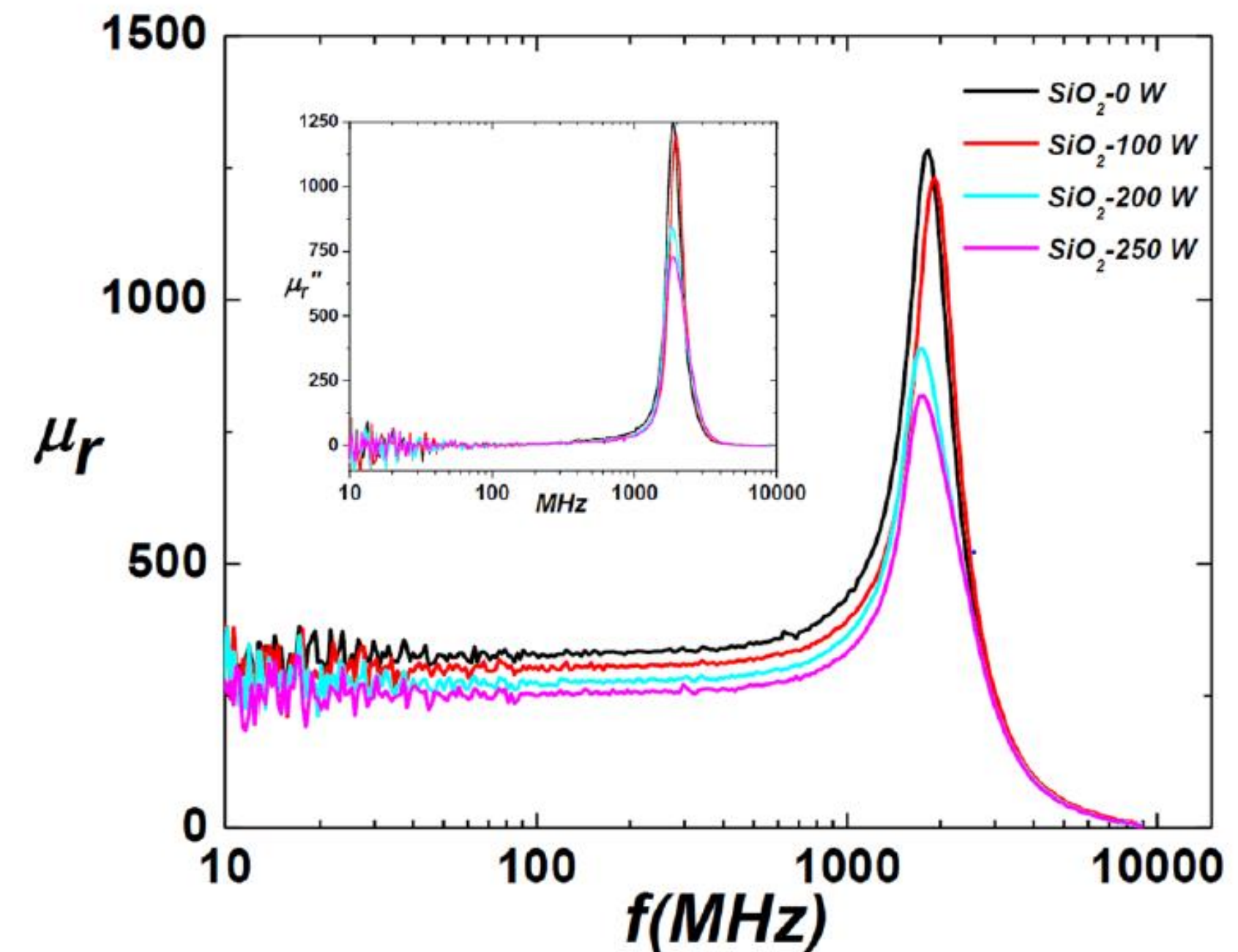


FIG. 8. The high-frequency permeability ( $\mu_r$ ) response of the CZTB-SiO<sub>2</sub> composite films deposited at different powers of SiO<sub>2</sub>. The inset presents the imaginary part ( $\mu_r''$ ) of the films.

SFI No. R17121 "Adept" Project

[7] Darragh Cronin et al., Tyndall



# Energy Harvesting, Ultra Low Power IoT Sensor Node

**Majority of ULP PMICs are *Boost* and the inductor value/size is relatively huge.**

> 10  $\mu$ A minimum average current and smaller cycle ripple peak currents (10 -100 mA pk.)

=> 10 – 22  $\mu$ H L value

Require low DCR for low voltage driving of the current ramp-up  $v(t) = R.i(t) + L.di(t)/dt$

**The topology for ULP requires development!**

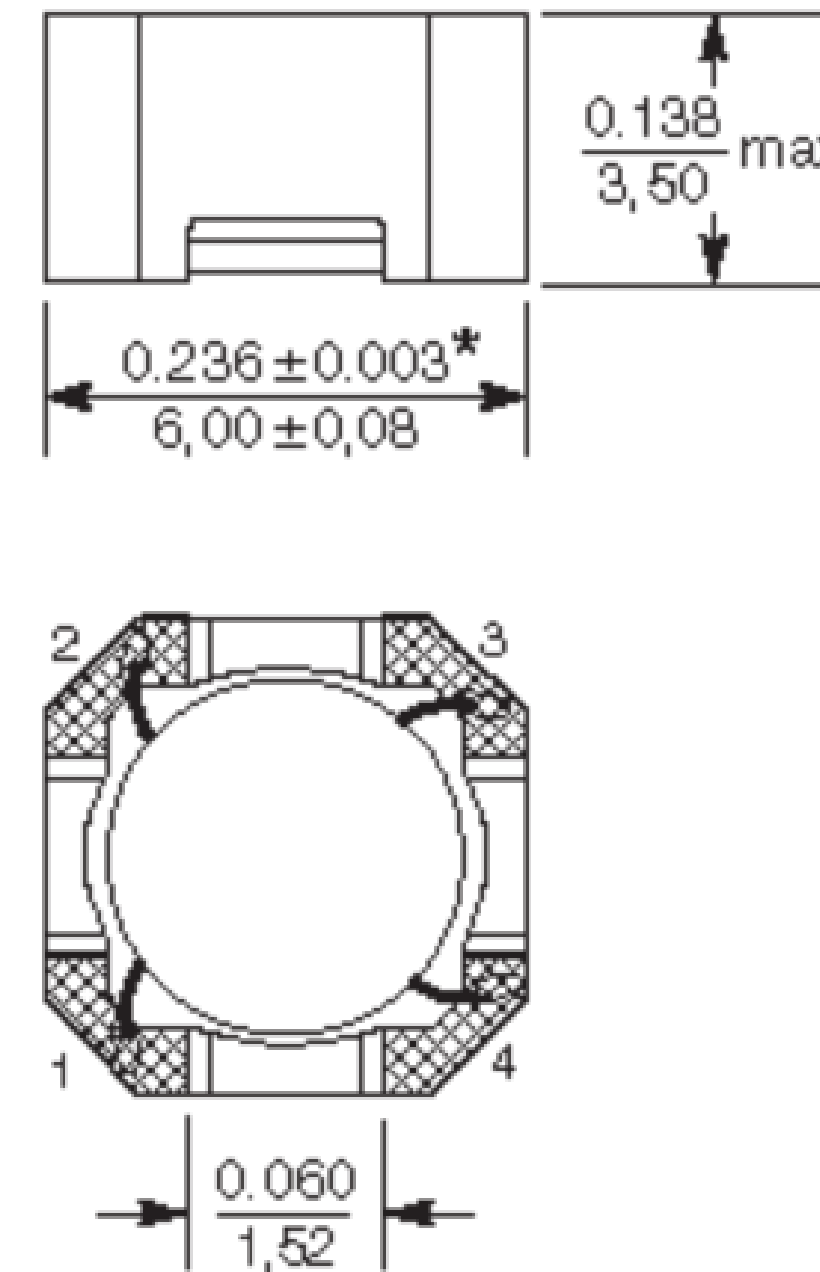
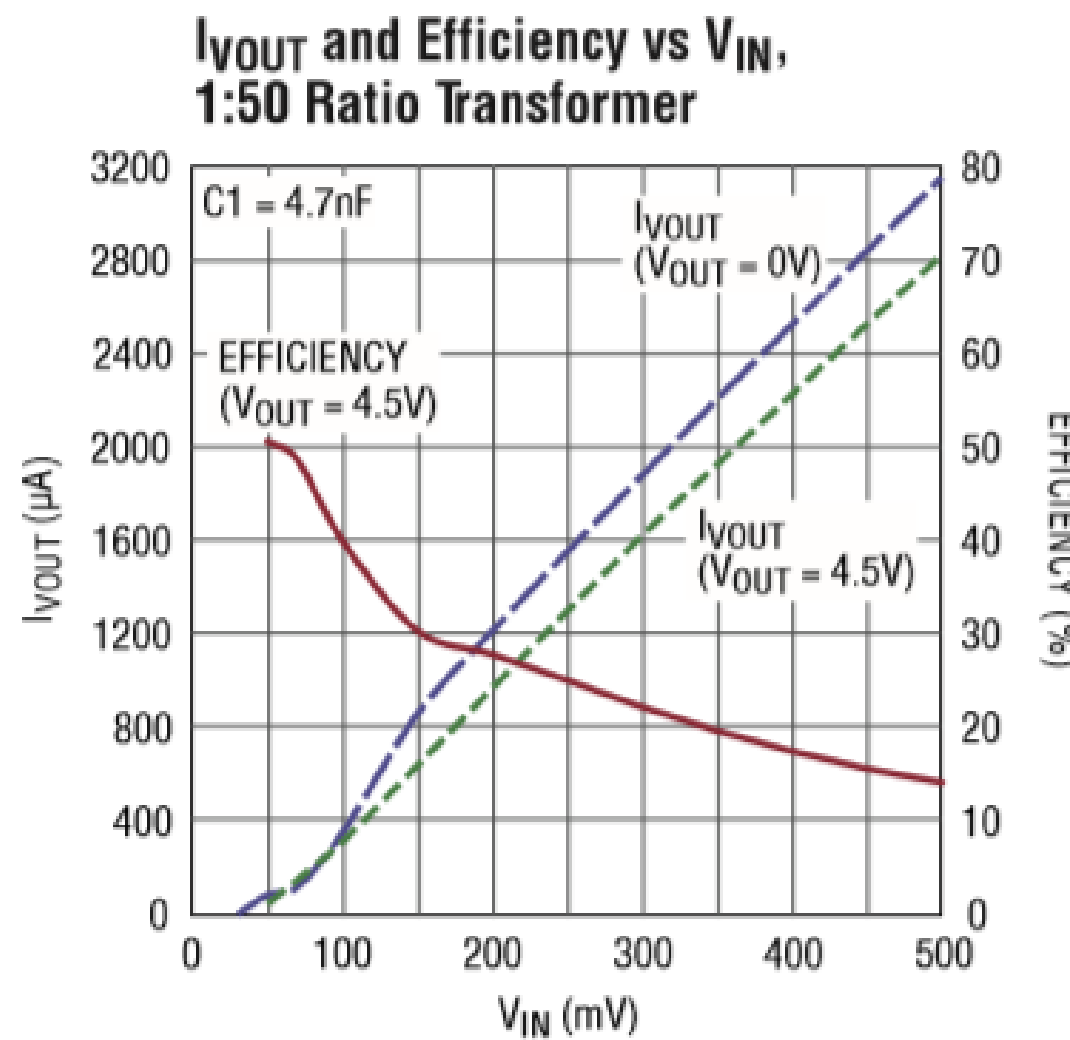
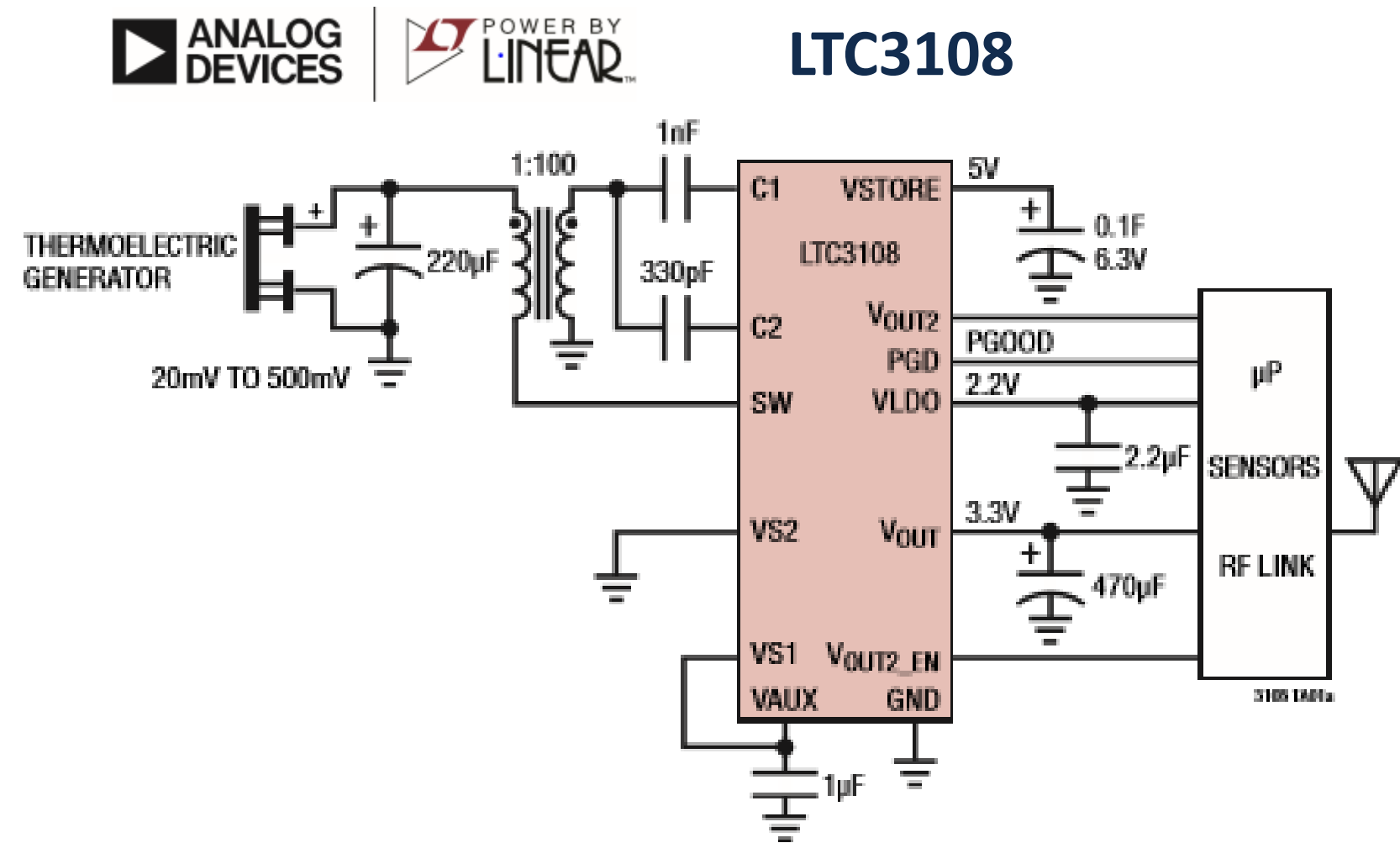
**For now we will look at the cold-start challenge.**

Ultra Low Power (high  $R_s$ ) is desirable; 3  $\mu$ W+ is commercially available ([www.e-peas.com](http://www.e-peas.com))

Ultra Low Voltage (for TEG) is desirable; 20 mV+ is commercially available



# Commercial Low Voltage Cold Start



1:100 Tx => Start-up at 20mV,  $I_{in} > 3\text{mA}$

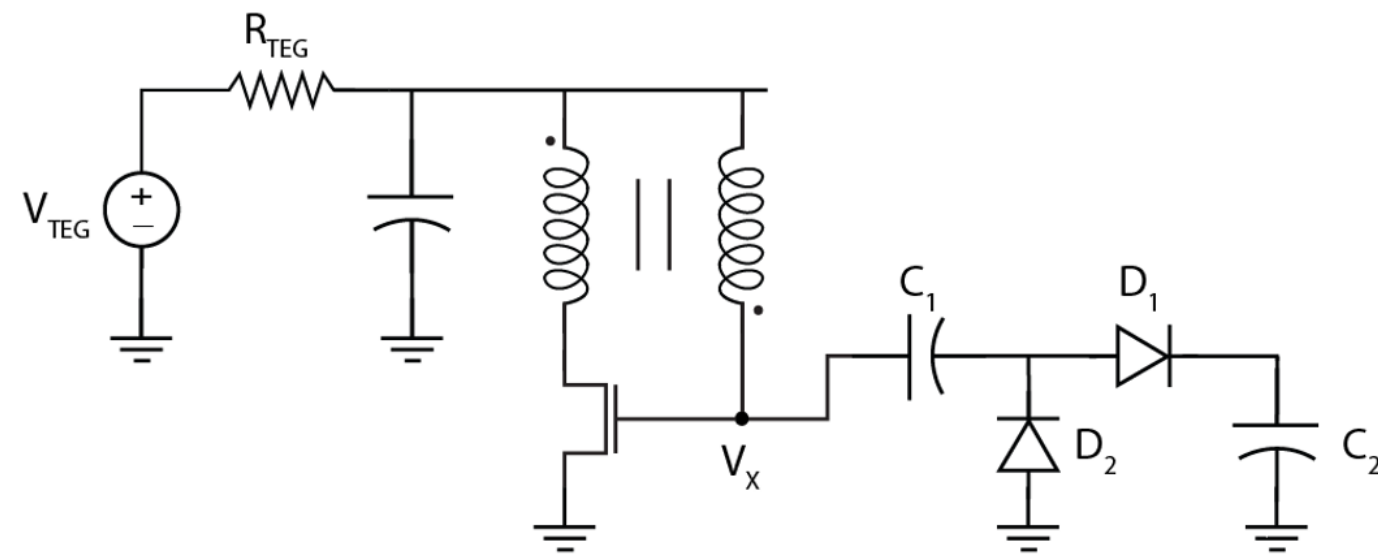
$f_0$  recommended 10 – 100 kHz

Resonant 1:N coupled-inductor is relatively huge at **6 X 6 X 3.5** mm

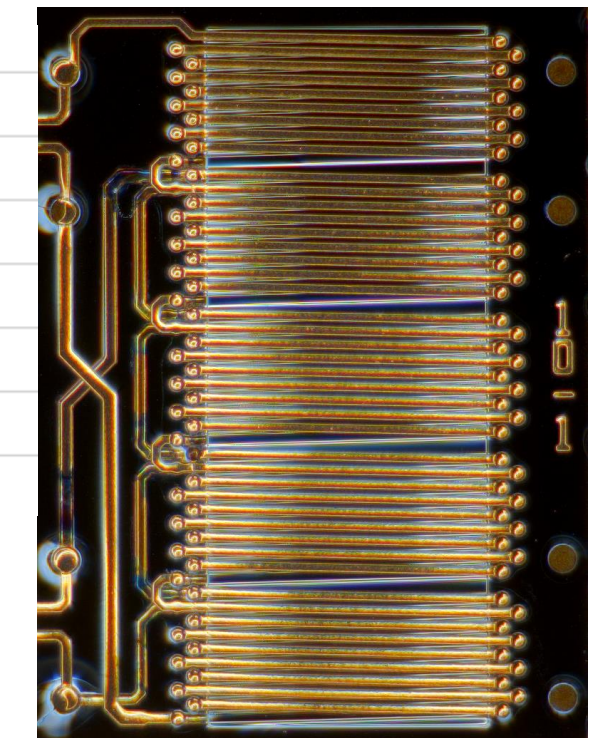
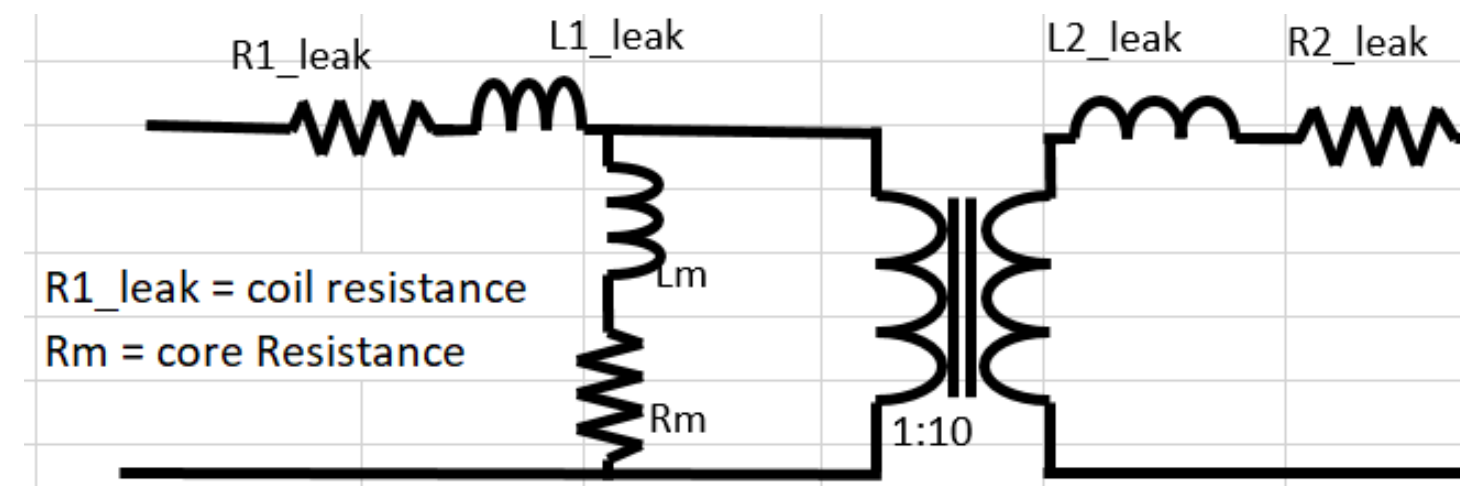
<https://www.analog.com/media/en/technical-documentation/data-sheets/LTC3108.pdf>



# 4:40 tf-MoS Meissner Oscillator based:



	100 Hz	15 MHz	20 MHz
Lm [nH]	4	16.4	18.7
L1_leak [nH]	4	19.2	19.1
L2_leak [nH]	100	90	80
Rm [Ohm]	0.001	0.261	0.972
R1_leak [Ohm]	0.049	0.53	0.568
R2_leak [Ohm]	0.8	6.7	7.8



Meissner Oscillator [12]

- 180 nm CMOS *simulation* using measured S Parameter Model:

14 MHz =  $f_0$

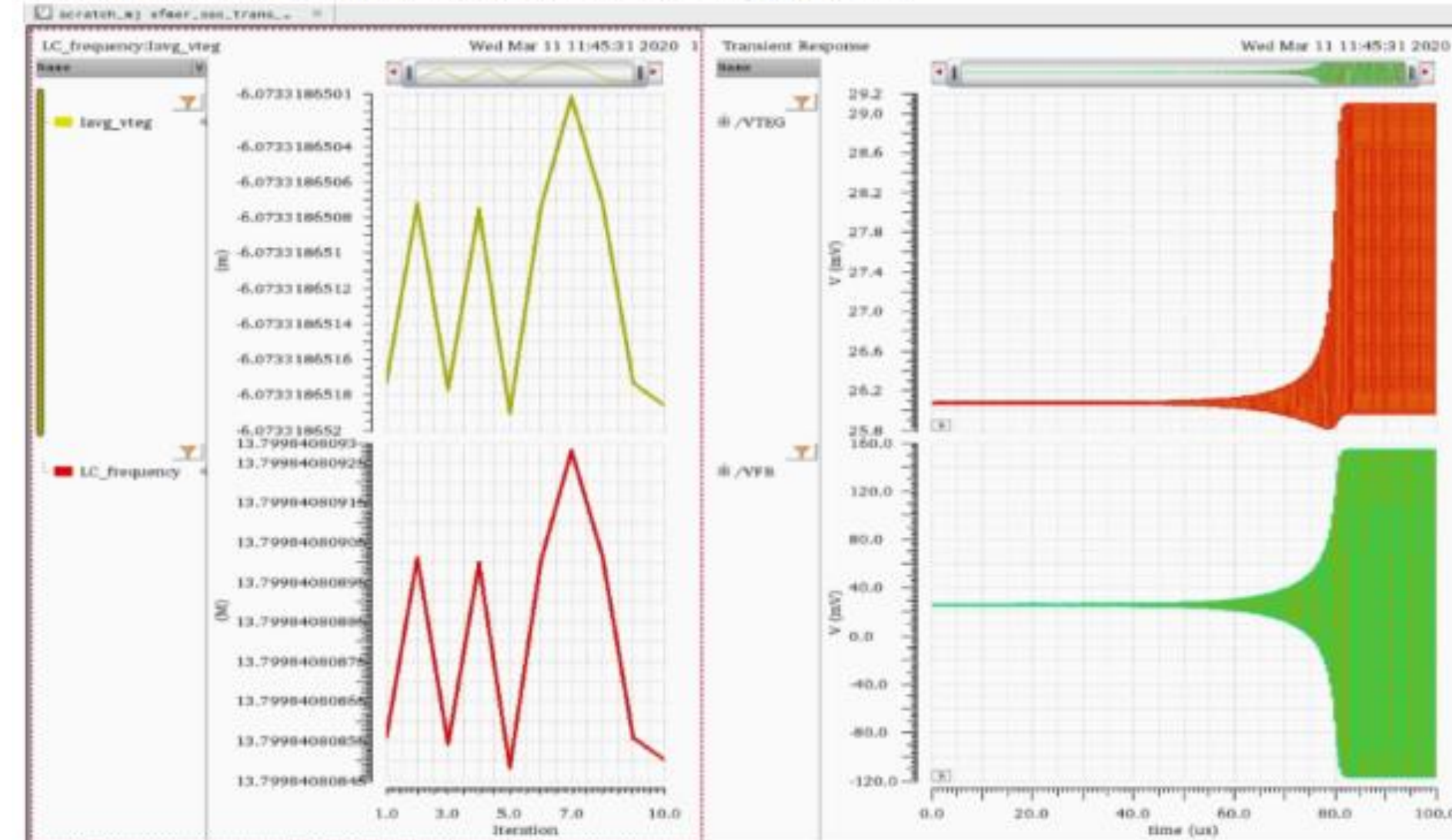
4.2 mA lin @ 30 mV (SCH)

200 X 100 um Dep.

Device

$k \sim 0.65$

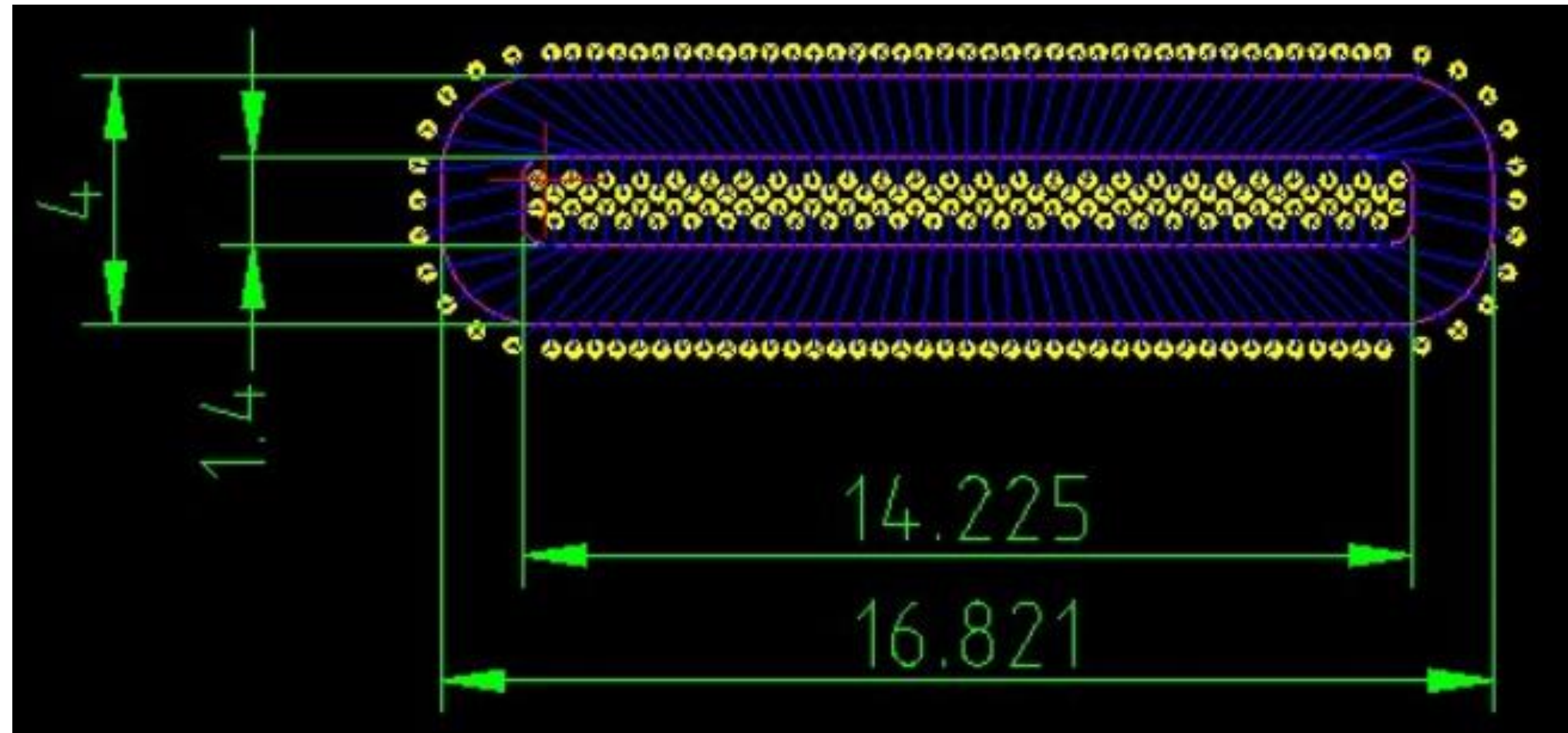
Transient noise simulation with TEG internal resistance = 0.5 Ohm; 10 iterations



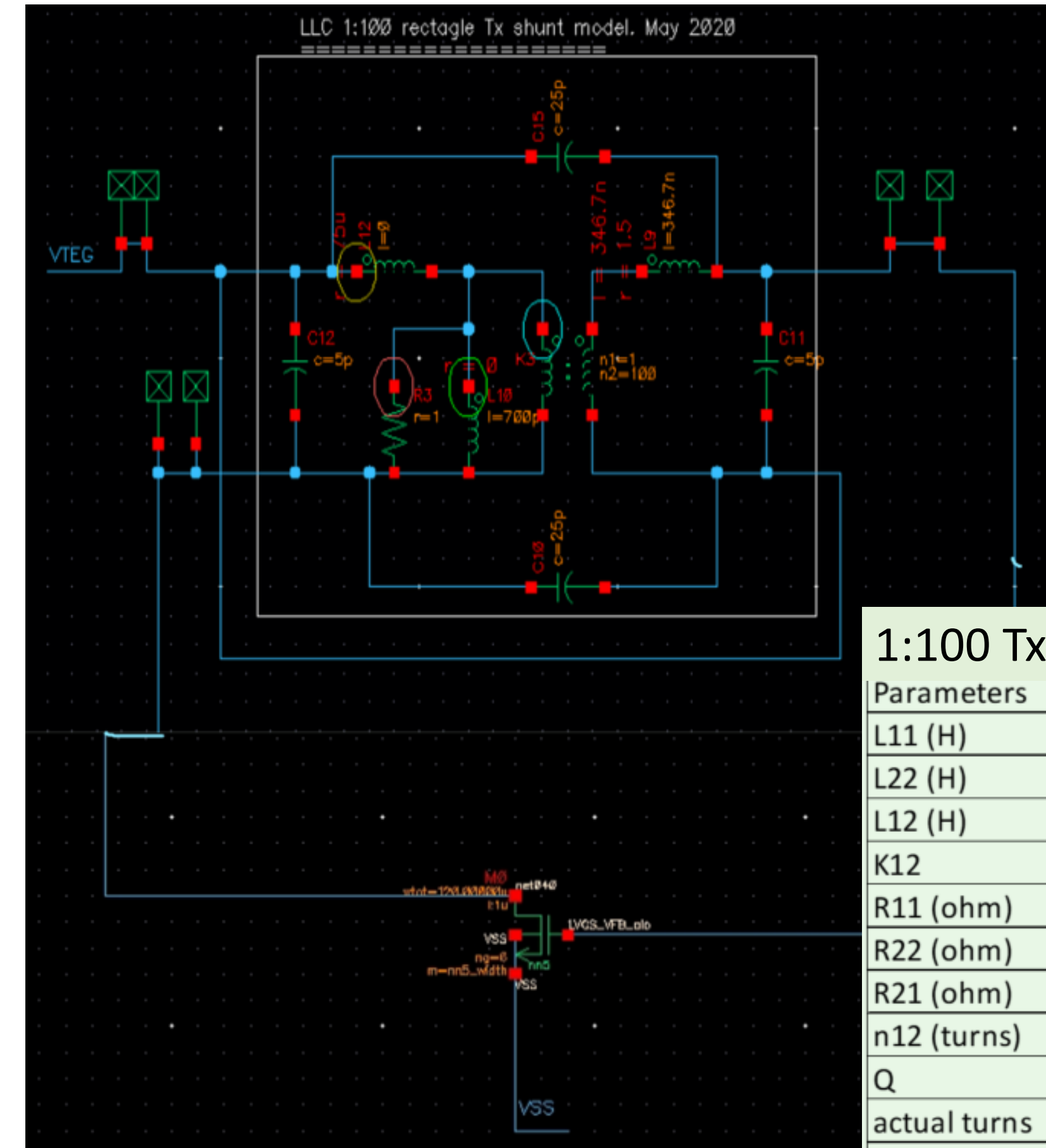
Feature	Dimension
Cu trace width	80 um
Cu trace thickness	16 um
Via diameter	100 um
Bond-pad diameter	160 um
Die size after dicing	4 x 5.2 mm <sup>2</sup>
Die size before dicing	4.6 x 5.9 mm <sup>2</sup>



# PCB Embedded Tx Meissner Oscillator



- 180 nm *simulation* (nn5 128x120um) using characterised device model for 1:95 Tx, 100 um film
- $I_{MAG} = 2\text{mA}$ ,  $I_{in} = 6.6\text{ mA}$ , 7.5 MHz,  $V_{in} = 15\text{mV}$  (SCH)
- Standard PCB Design Rules, 35  $\mu\text{m}$  Cu
- 3M EM15TF ferrite sheet;  $\mu_r = 150$
- Very large path length,  $I_e$  !
- Single 3M film gives 5 X  $L_{MAG}$  and 3 X Size vs MoS



1:100 Tx Model	
Parameters	
L11 (H)	6.93548E-10
L22 (H)	6.93548E-06
L12 (H)	6.5887E-08
K12	0.95
R11 (ohm)	2.25E-03
R22 (ohm)	2.33E+01
R21 (ohm)	2.18E+01
n12 (turns)	100
Q	20
actual turns	95

**EnABLES** EU H2020 Grant No. 730957



# 1:1 MoS Gate Driver Signal Tx (MoS GD Tx)

Galvanic Isolation 1 - 5 kV for Primary-Side/Functional Isolation (Operational Insulation per IEC950)



Signals and isolated bias for flying Gate-Driver/Control Telemetry in the Smart Switch Application

10 V.ns application, 40 nH  $L_{MAG}$

48 to 1 V POL

Multi-Level Converters with 20 - 200 V cells

Primary bridge drives for wireless power transfer

Resonant bias supplies

Secondary-side SR drives

Measured Tx parameters match FEM simulated

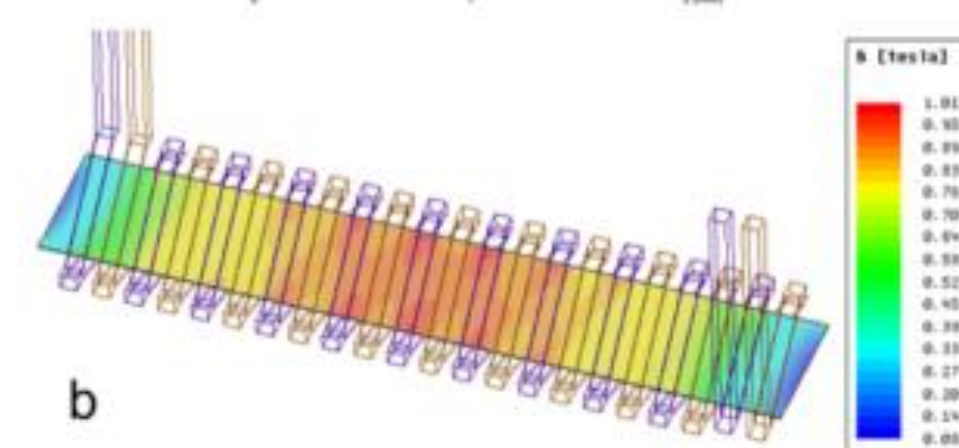
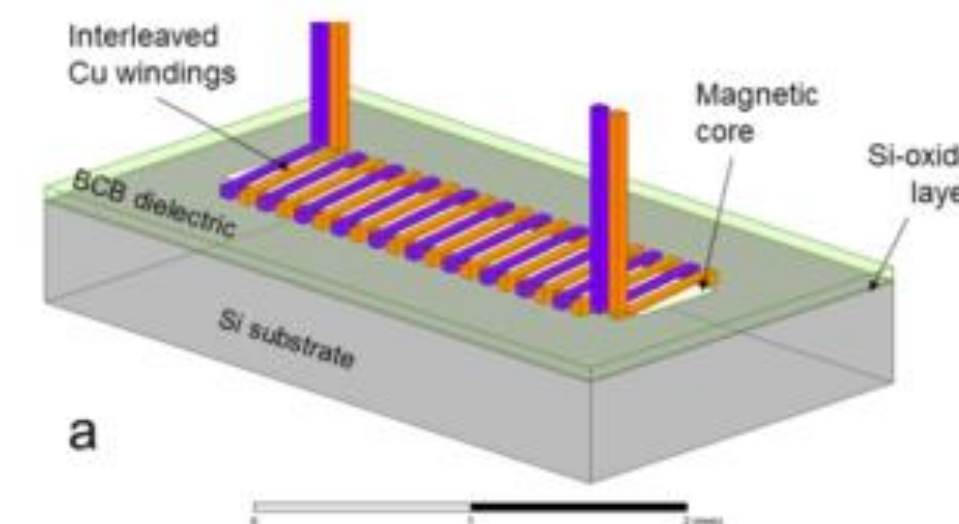
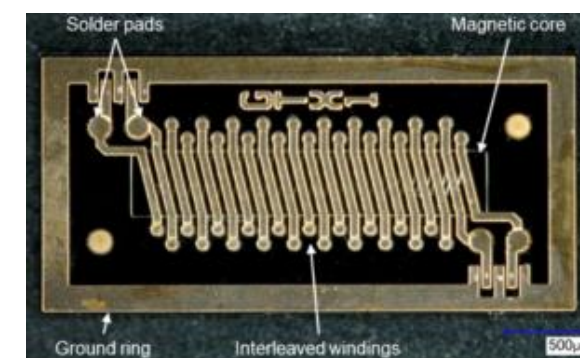
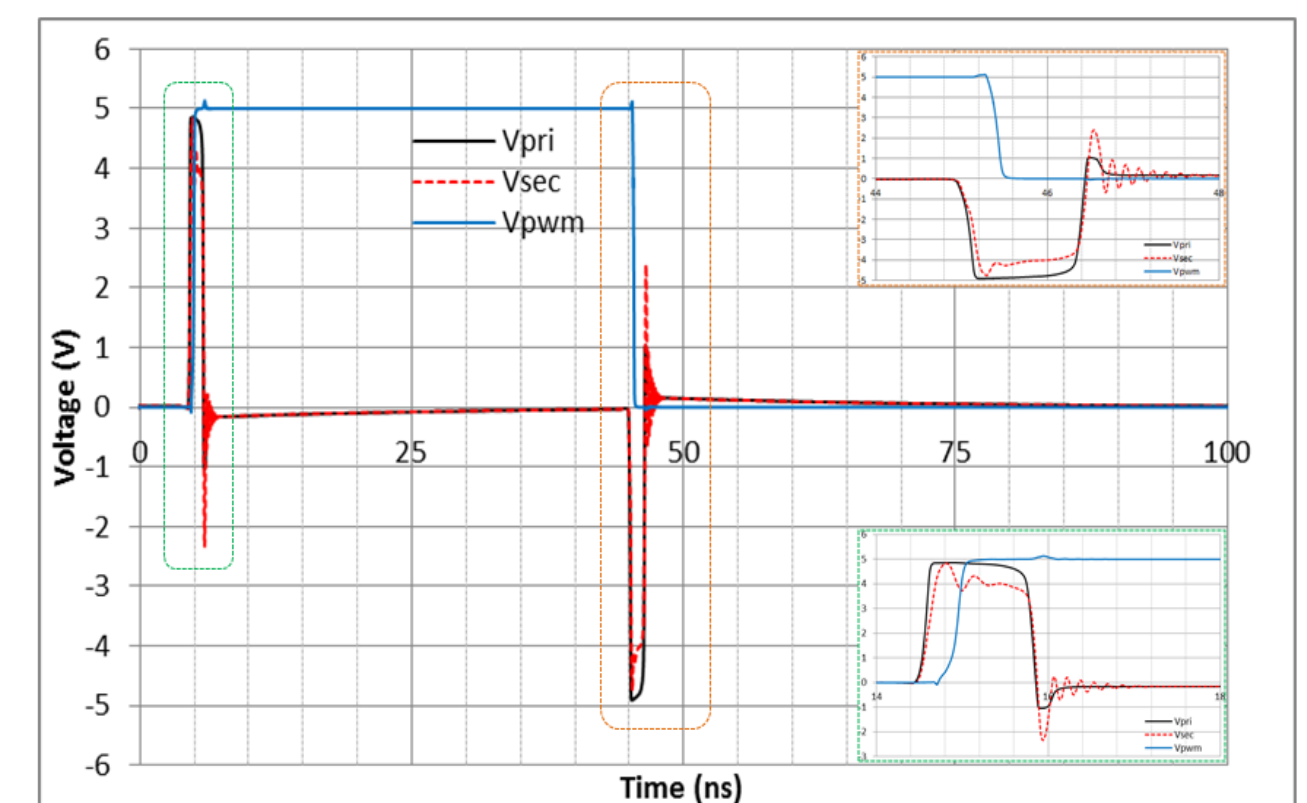


Table 2 Summary of FEM simulation results

Parameter	Values	
Switching frequency ( $f_{SW}$ ) [MHz]	20	
Magnetizing inductance ( $L_{11}$ ) @ $f_{SW}$ [nH]	39.3	
Coupling coefficient ( $k_{12}$ )	0.83	
DC resistance ( $R_{DC}$ ) [mΩ]	310	
Quality factor @ $f_{SW}$	13.7	
Si-oxide base thickness [μm]	1	5
Parasitic capacitance ( $C_{12}$ ) [pF]	10.76	3.68



Simulated for 130 nm CMOS

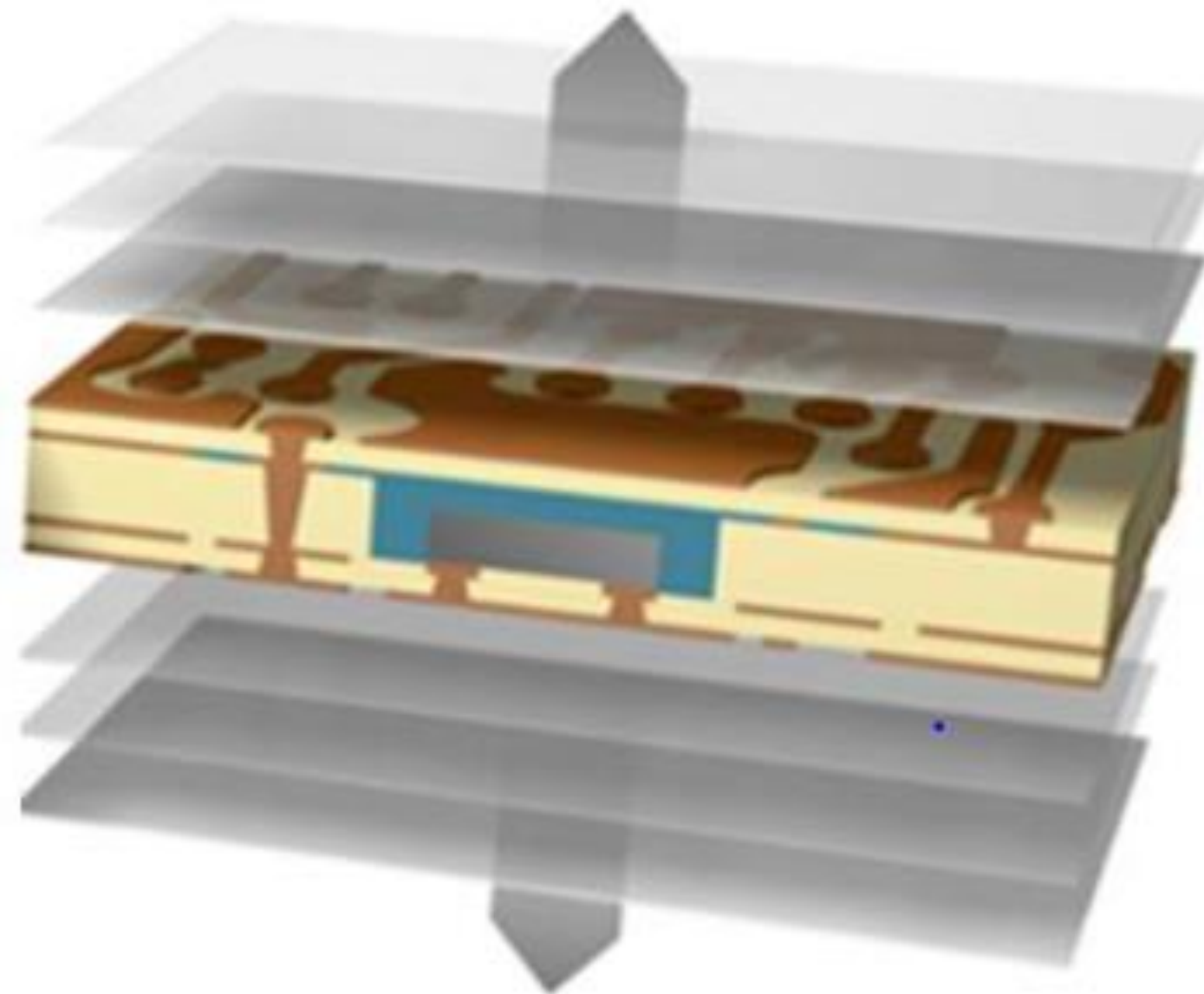
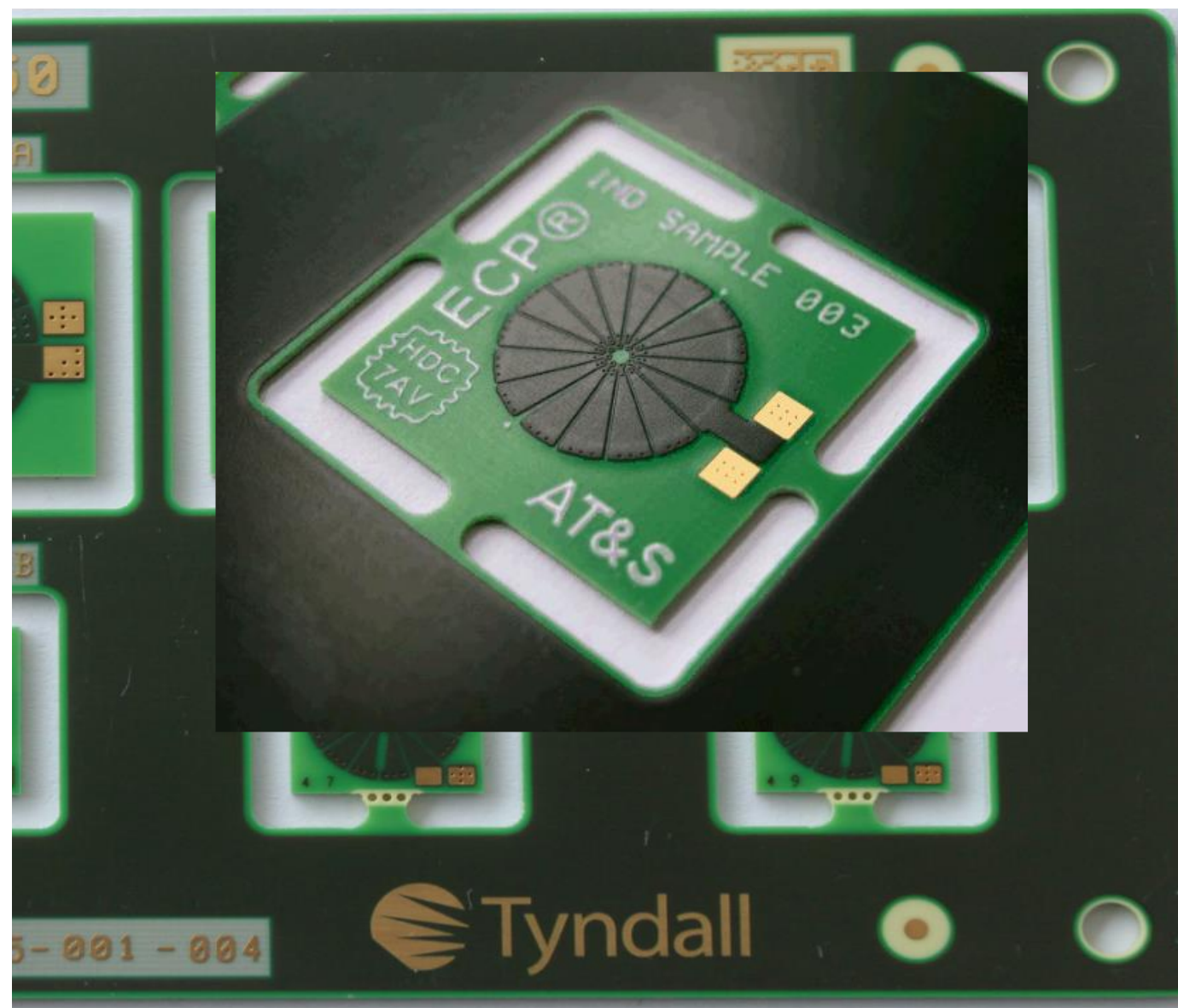
[8] Z. Pavlovic, Tyndall, et al. EU H2020 "GaNonCMOS" [www.ganoncmos.eu](http://www.ganoncmos.eu)



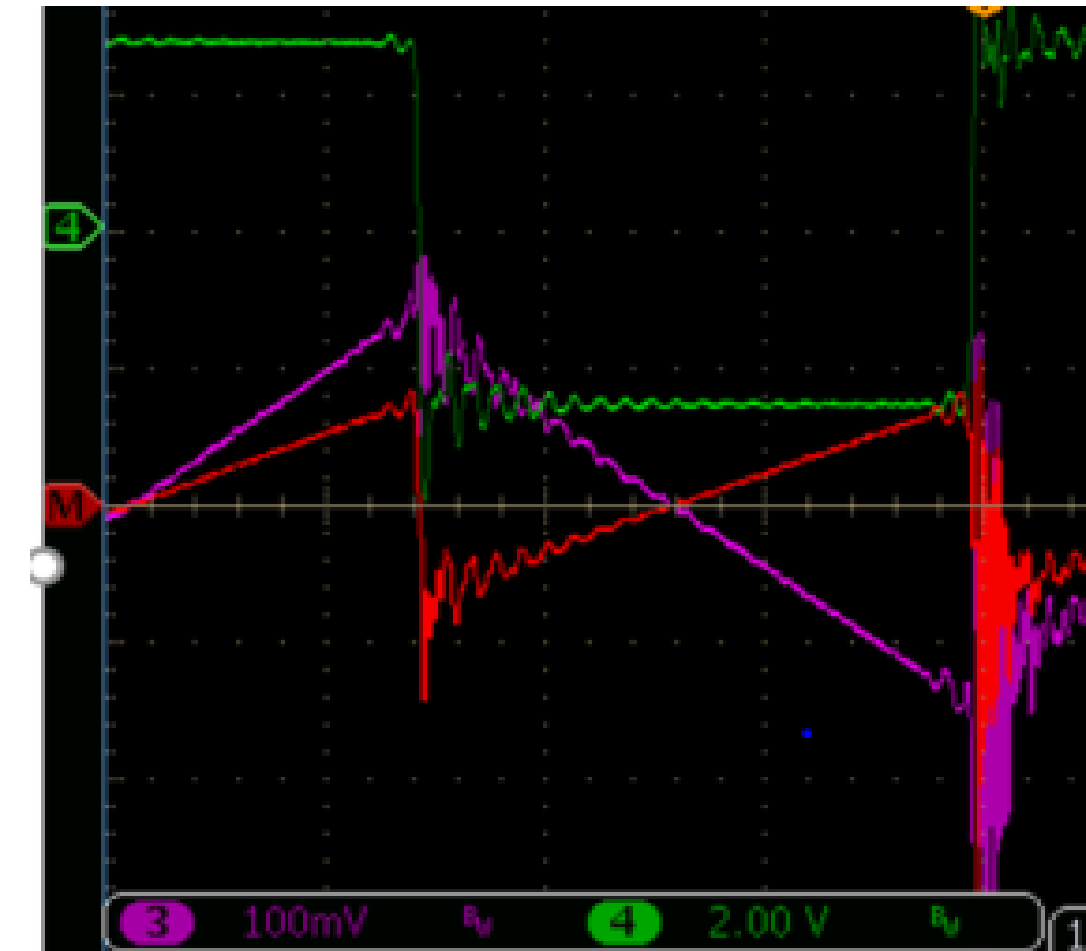
# Characterisation of Substrate Embeddable Materials

$Q_{Isic}$  Large signal in-converter Q.

Particularly elucidating regarding intrinsic material capacitances, HF magnetic loss damping, EMI impact, B-H loop tracing,..

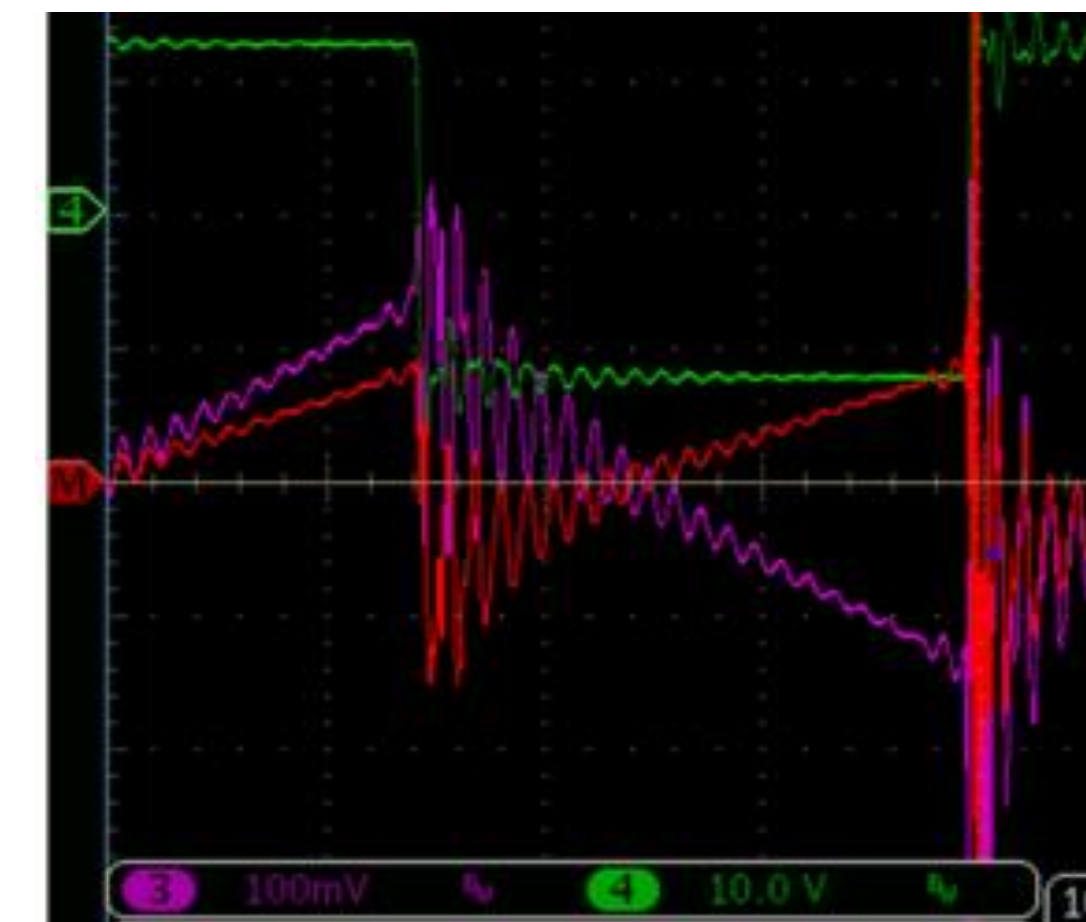


Centre Core Embedding,  
CCE, AT&S



Ferrite particles in post cure resin

$V_L$  (green),  
 $I_L$  (purple)  
 $V_L \cdot I_L$



Metal sheets in resin

[9] R. Murphy, Tyndall, et al., G. Weidinger et al., AT&S, EU H2020 "GaNonCMOS" [www.ganoncmos.eu](http://www.ganoncmos.eu)





# Commercial Magnetic Materials Characterisation & Embedding Qualification



[www.ganoncmos.eu](http://www.ganoncmos.eu)

“GaN CMOS” program with AT&S: a variety of new materials are emerging, which are suitable for embedding and exiting reliability trials

Sintered ferrites (some are parylene coated)

Ferrite loaded epoxies, polymers

Magnetic particles in polymer

Laminated metallic strips in polymer

Flex sheets with ferrite powders

Embedded Tyndall thin film CZT(B)

Some materials will marginally advance the 9 MHz **Performance Factor** achieved by low permeability ferrite, Alex Hanson et al. in 2016 [10] – these still appear to be ferrite based!

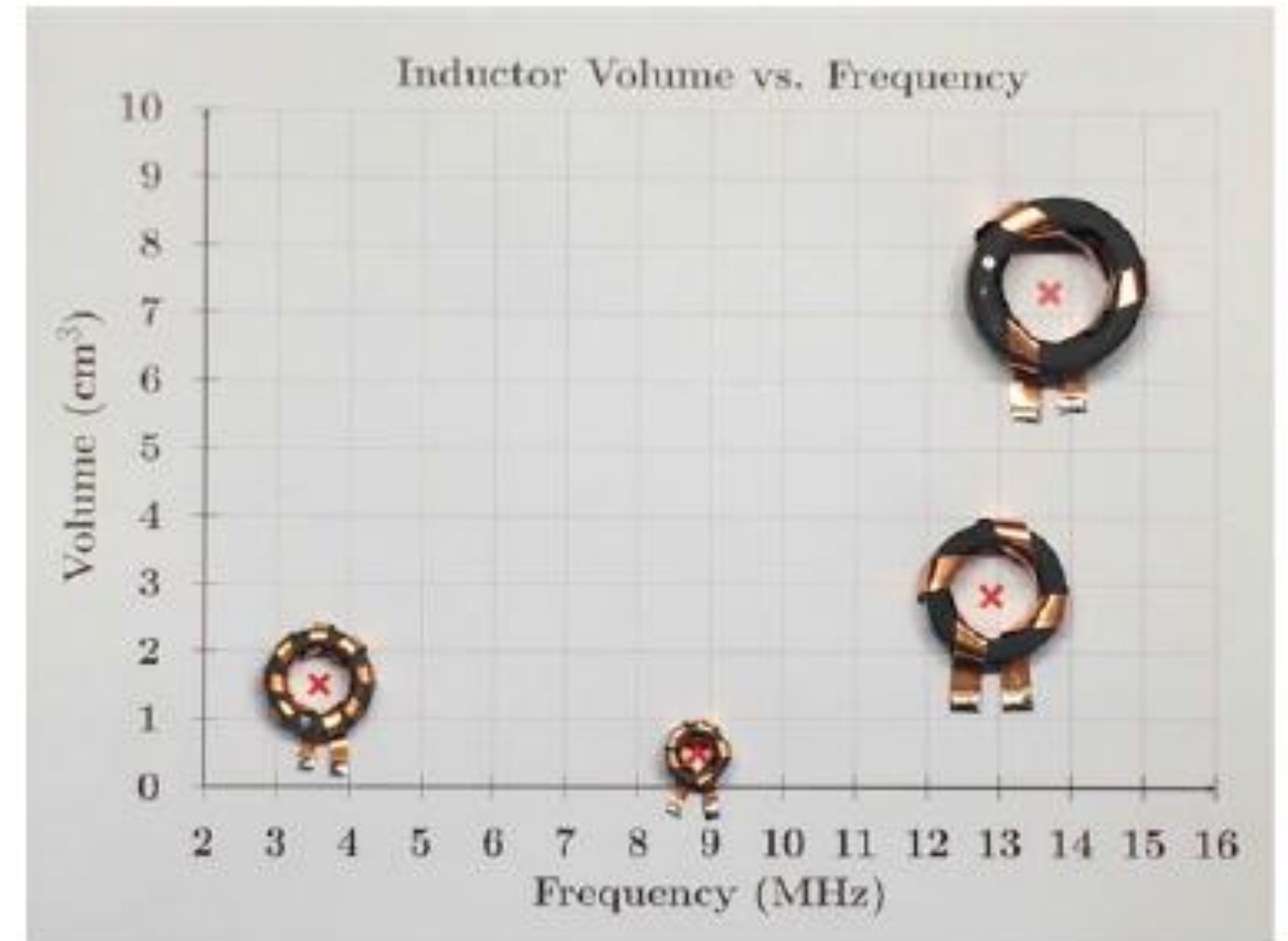


Fig. 4. Inductors using ungapped toroidal cores of Fair-Rite 67 material [10] Alex Hanson et al.,  $\mu_r = 40$



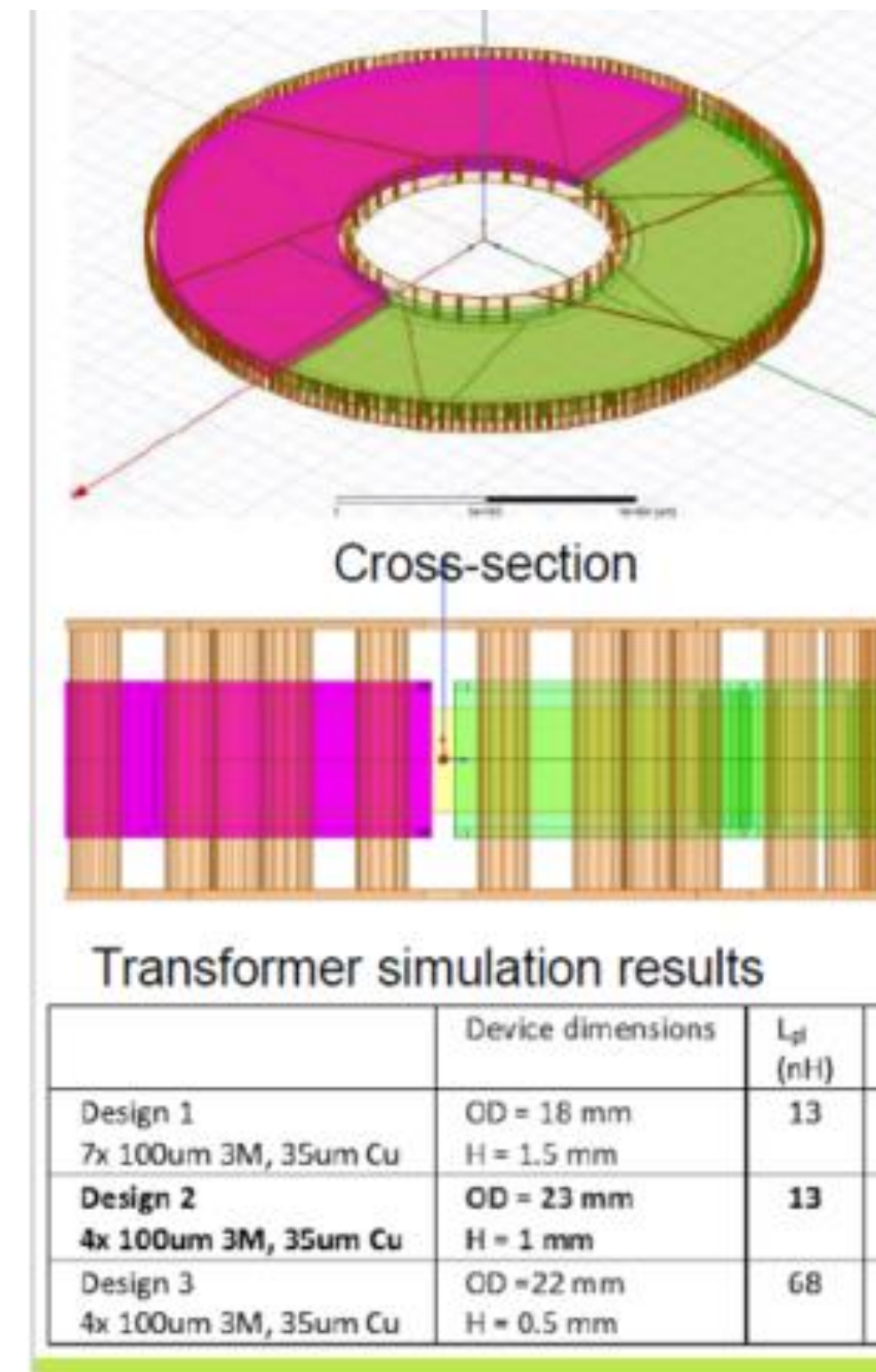
# Embedded 6:1:1 LLC Transformer Design

300 nH  $L_{MAG}$ , 30 nH Leakage Resonance, 95% target at 10 MHz, 2.5A DC output.

Embedded commercial material, 3M15TF, achieves large signal  $Q = 20$  at 10 MHz

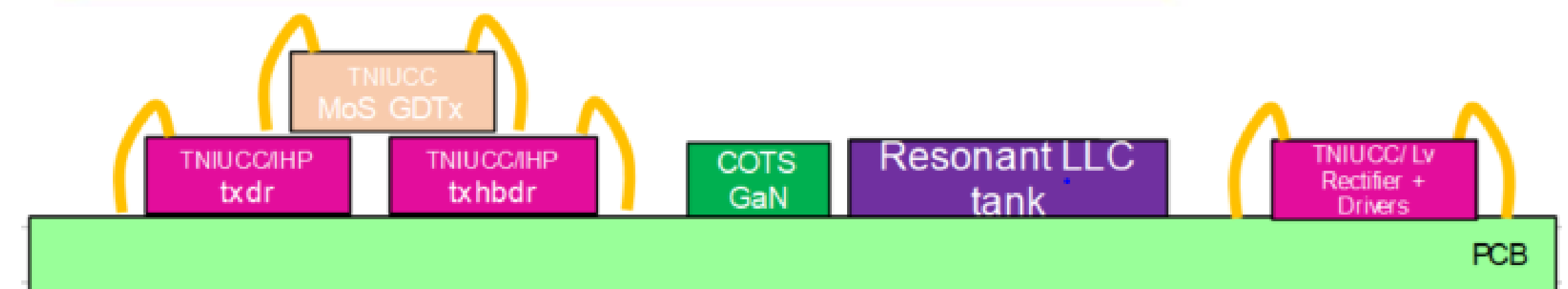
Up to 4 sheets of 0.1mm film compatible with standard PCB core thickness

LLC design comprises 5 V rated SR's and GaN primary switches all driven by MoS GD Tx



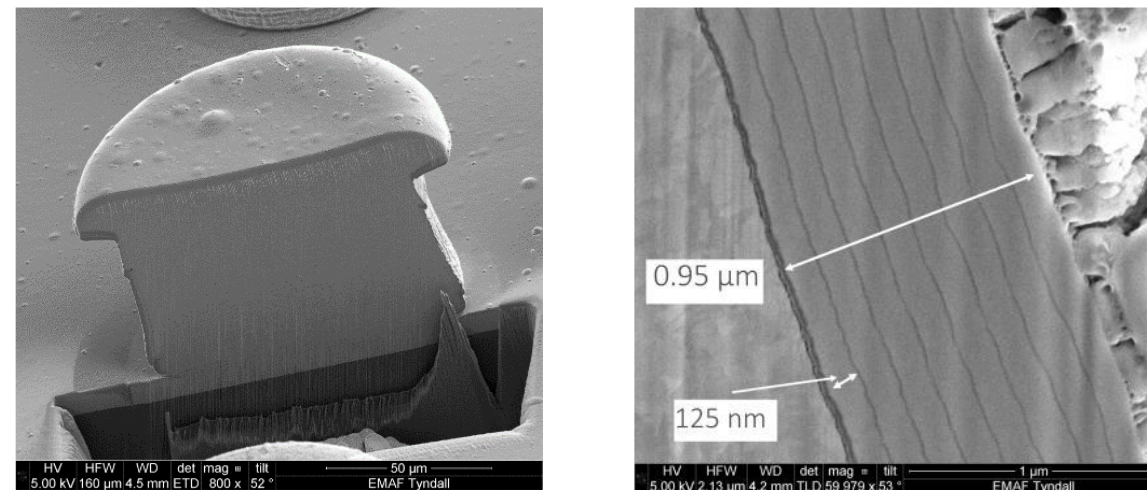
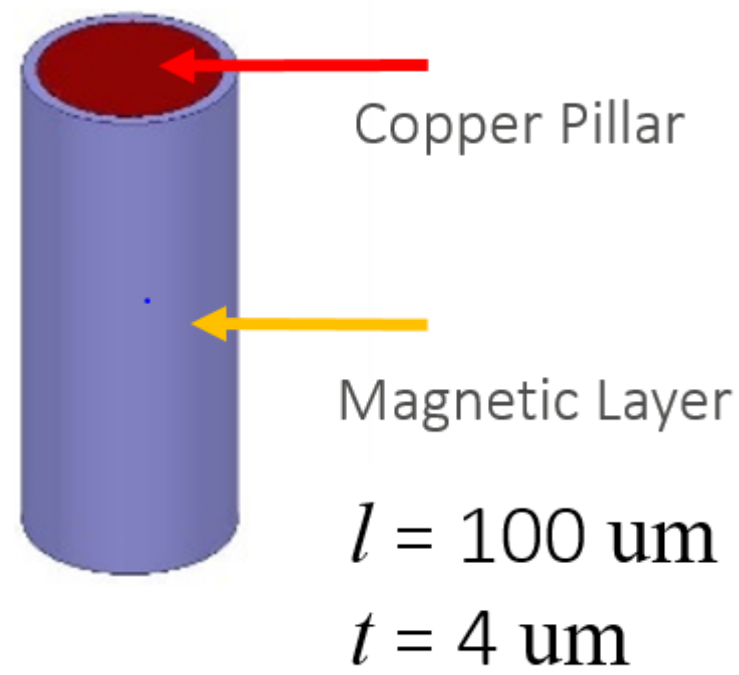
LLC Transformer modelled in Maxwell with Large signal material-in - device measured  $Q = 20$  at 10 MHz, 17 mT.

WP = brown, WS = pink, green





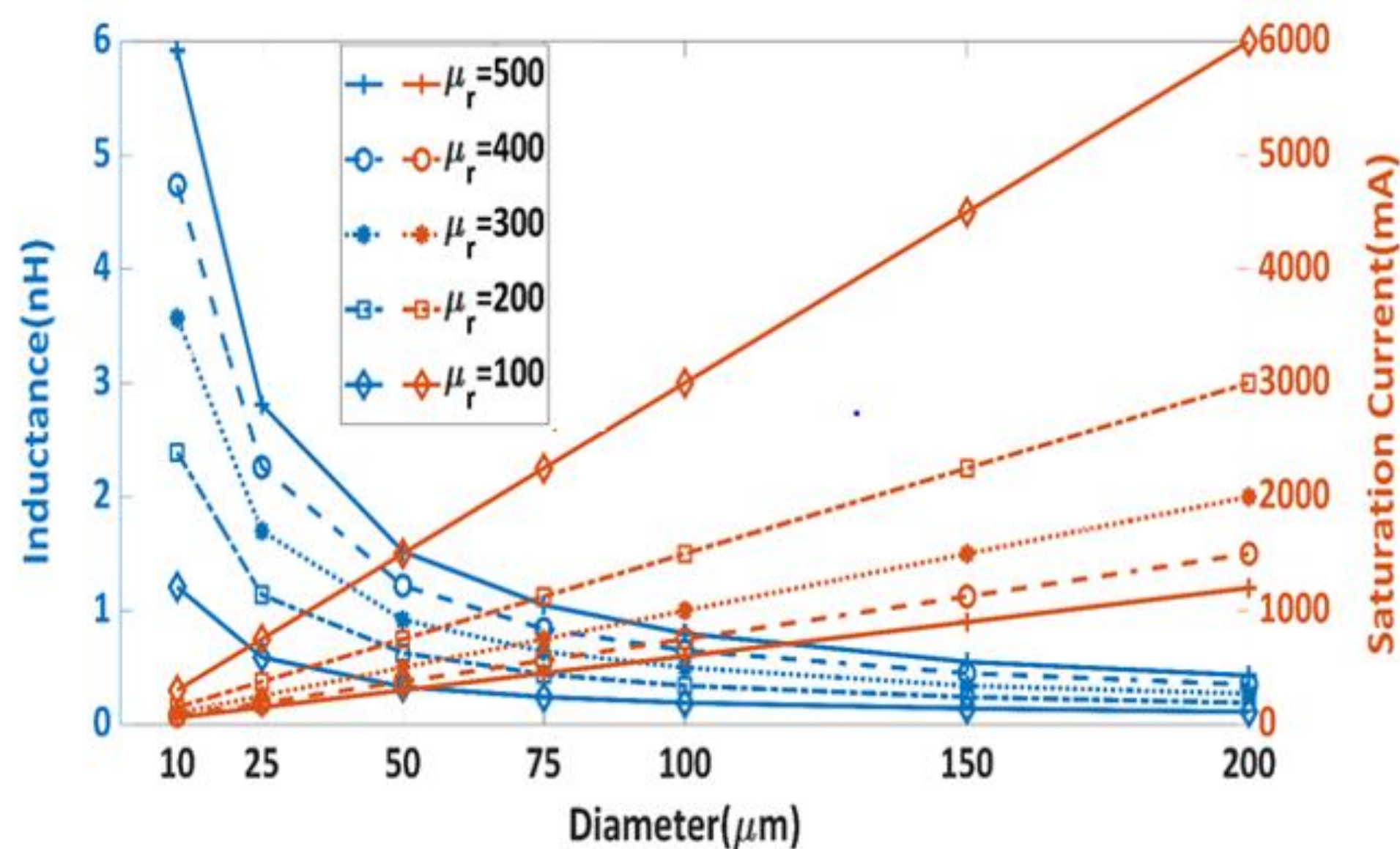
# Vertical Inductors Array for SoC iVR



Vertical Interconnect

- Increasing pillar aspect ratio (& L value) adds value for high phase count
- 6 A/mm<sup>2</sup> – area match-up with 28 nm CMOS VR power switching bridge

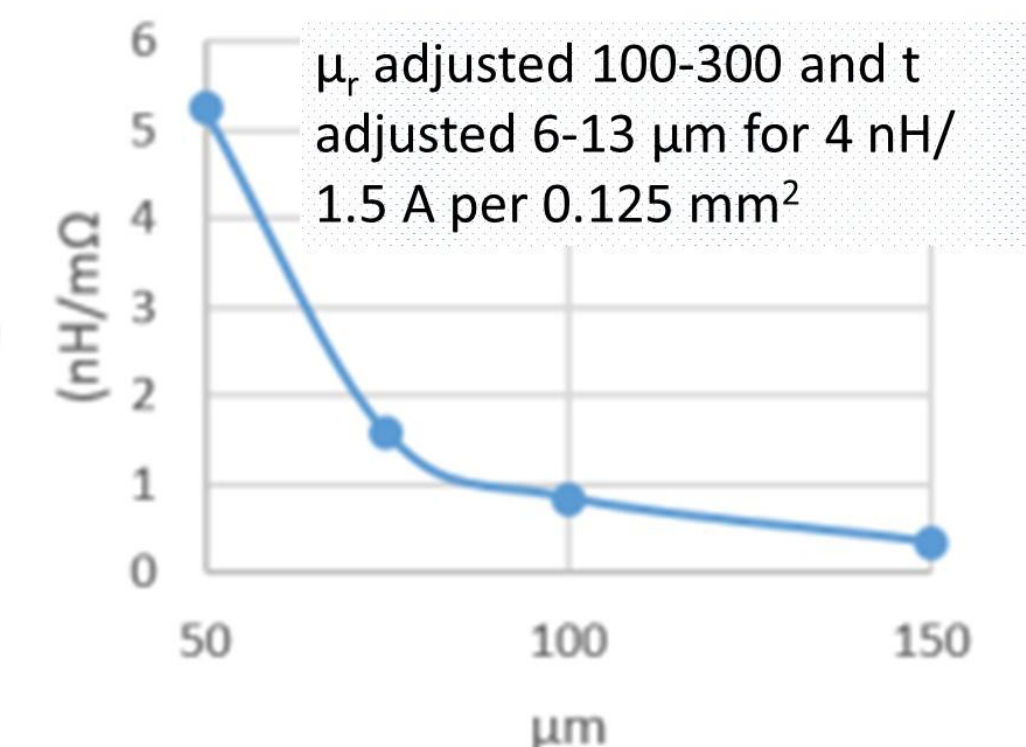
- High Saturation Current (N=1)  $I_{sat} = \frac{B_{sat}l}{N\mu}$
- Other TSV inductor systems, N>=1



Types	Solenoid (2D)	Adept 3D (Aircore)	Existing TSV Inductor [11]	Adept 3D Inductor	SMT 0402-0805 CHIP INDUCTOR <sup>3</sup>
Inductance Density (nH/mm <sup>2</sup> )	15	3.5	91	32 <sup>1</sup> 4 <sup>2</sup>	53
L (nH)/DCR(mΩ)	0.6	0.16	0.002	5.24	0.61
Current Density (A <sub>DC</sub> /mm <sup>2</sup> )	<1	*	1	0.75 <sup>1</sup> 6 <sup>2</sup>	1.23

<sup>1</sup> series, <sup>2</sup> parallel

Design Space Study  
L/DCR versus Diameter



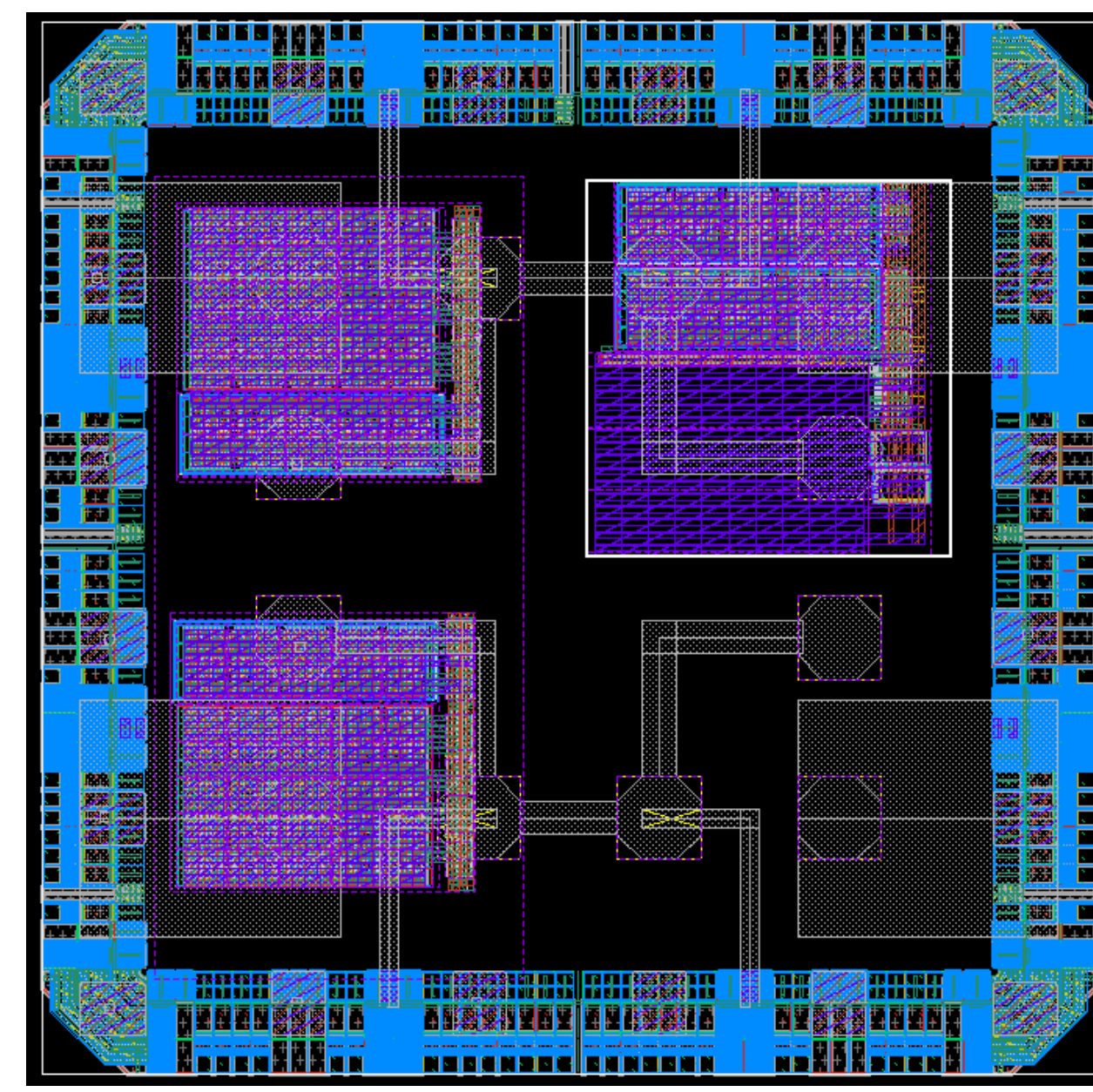
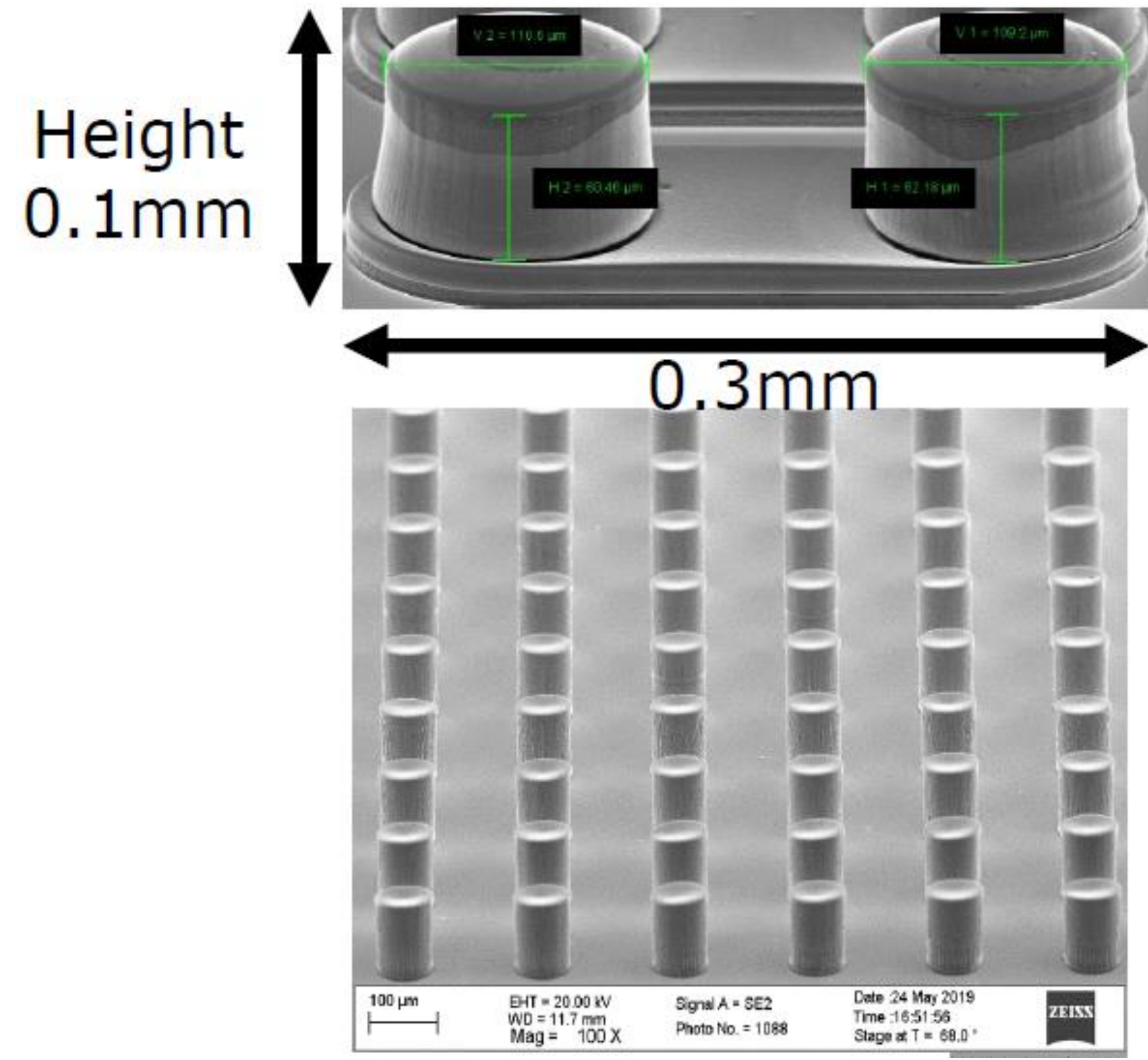
C. O' Mathúna et al., Science Foundation Ireland ADEPT Project –2017-2020



# Tyndall Vertical Inductors Array

~3 nH/pillar

Designed for Tyndall ([www.mcci.ie](http://www.mcci.ie))  
28 nm iVR; 4nH , 0.75ADC per phase,  
0.125 mm<sup>2</sup> power switch



1 X 1 mm 28 nm  
PMIC test-chip  
with PN Buck for  
88%, 100MHz,  
0.75A per  
0.125mm<sup>2</sup> block

C. O' Mathúna et al., Science Foundation Ireland  
ADEPT Project –2017-2020



# Conclusions

The laminated thin film CZT(B) planar solenoidal inductor offers a high Q (95+%) inductor solution over 10-100+ MHz

> 6X inductance density improvement over air-core for 10 nH +

Inductance density and L/R ratio improve with scaling for higher phase count

Solution size reduction with inverse-coupling and multi-level for optimum duty cycle set

PCB/Substrate/Interposer embedding of *stacks* of laminated thin films offers the prospect of **low DCR** & relatively **high  $L_{MAG}$**  & **10 – 100 MHz** inductor devices

High frequency transformer (higher permeability/ $L_{MAG}$ ) based applications such as LV cold-start and resonant bias appear well suited to PCB embedding or tf-MoS for areas such as EH IoT.

The vertical inductors array could offer attractive parameters such as  $I_{SAT}$ , DCR in packaging systems which exploit 3-D



# Acknowledging

*Paul McCloskey, Cian O'Mathúna, Michael Hayes, [www.mcci.ie](http://www.mcci.ie)*



*GaNonCMOS project partners, [www.ganoncmos.eu](http://www.ganoncmos.eu)*



# References

- [1] J. Lopez, C. Fernandez, P. Zumel, S. O. Driscoll, and C. O'Mathuna, "Integrated inductor optimization for Power Supply on Chip," in 2018 IEEE 19th Workshop on Control and Modeling for Power Electronics (COMPEL), pp. 1–6, IEEE, 2018.
- [2] "Electrical Characterisation of Thin Film CZTB Solenoid Inductors for PwrSiP", Pranay Podder et al. IEEE PwrSoC 2018
- [3] "Ultra-low loss integrated magnetics platform for high frequency power delivery networks", Pranay Podder et al., Tyndall, Chor Shu Cheng et al., Global Foundries, 11<sup>th</sup> International Conference on Integrated Power Electronic Systems; Berlin, Germany. March 24-26th, 2020
- [4] "Comparison of Coupled vs. Non-Coupled Microfabricated Inductors in 2W 20MHz Interleaved Buck Converter", Youssef Kandeel, NUIG, et al. APEC 2019
- [5] Zhara Ghaferi et al, "Characterization and enhancement of magnetic performance of electrodeposited Ni<sub>45</sub>Fe<sub>55</sub> on PCB for high frequency application", Journal of Magnetism and Magnetic Materials (2020)



# References

[6] D. Jordan et al, “High Q-Factor PCB Embedded Flip-Chip Inductors with Multi-Layer CZTB Magnetic Sheet for Power Supply in Package (PwrSiP)”, DOI 10.1109/JESTPE.2020.2983125

[7] D. Cronin et al., “Soft magnetic nanocomposite CoZrTaB–SiO<sub>2</sub> thin films for high-frequency applications”, J. Applied Physics (2020)

[8] “Thin-film Magnetics-on-Silicon Integrated Transformer for Isolated Signal and Power Coupling Applications”, Zoran Pavlovic et al., 11th International Conference on Integrated Power Electronic Systems; Berlin, Germany. March24-26th, 2020

[9] “ PCB Embedded Toroidal Inductor for 2MHz Point-of-Load Converter”, Ruaidhrí Murphy, Tyndall et al., Gerald Weidinger, AT&S, 11<sup>th</sup> International Conference on Integrated Power Electronic Systems; Berlin, Germany. March24-26th, 2020

# References

[10] “Measurements and Performance Factor Comparisons of Magnetic Materials at High Frequency”, Alex Hanson et al., IEEE TRANSACTIONS ON POWER ELECTRONICS, VOL. 31, NO. 11, NOVEMBER 2016

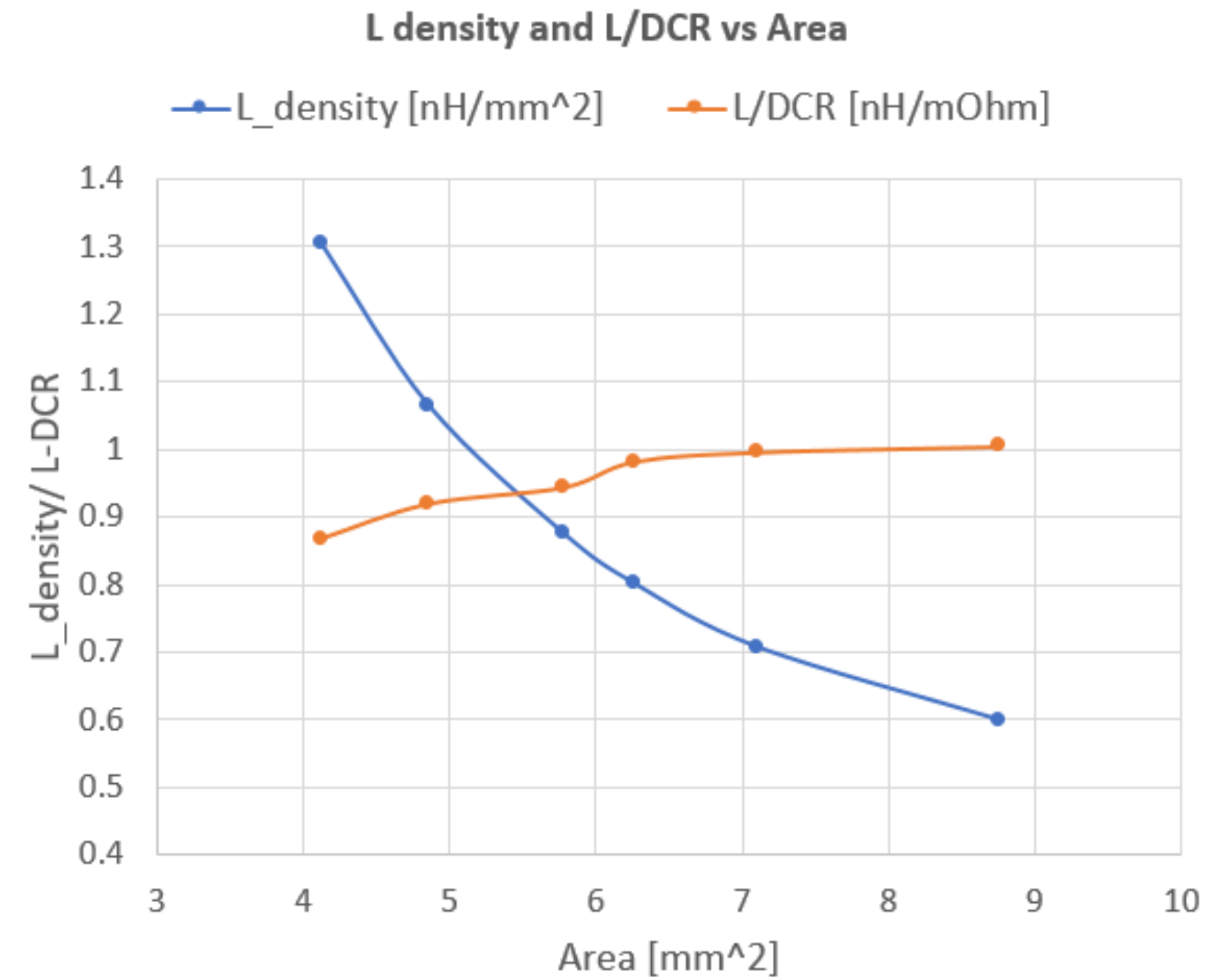
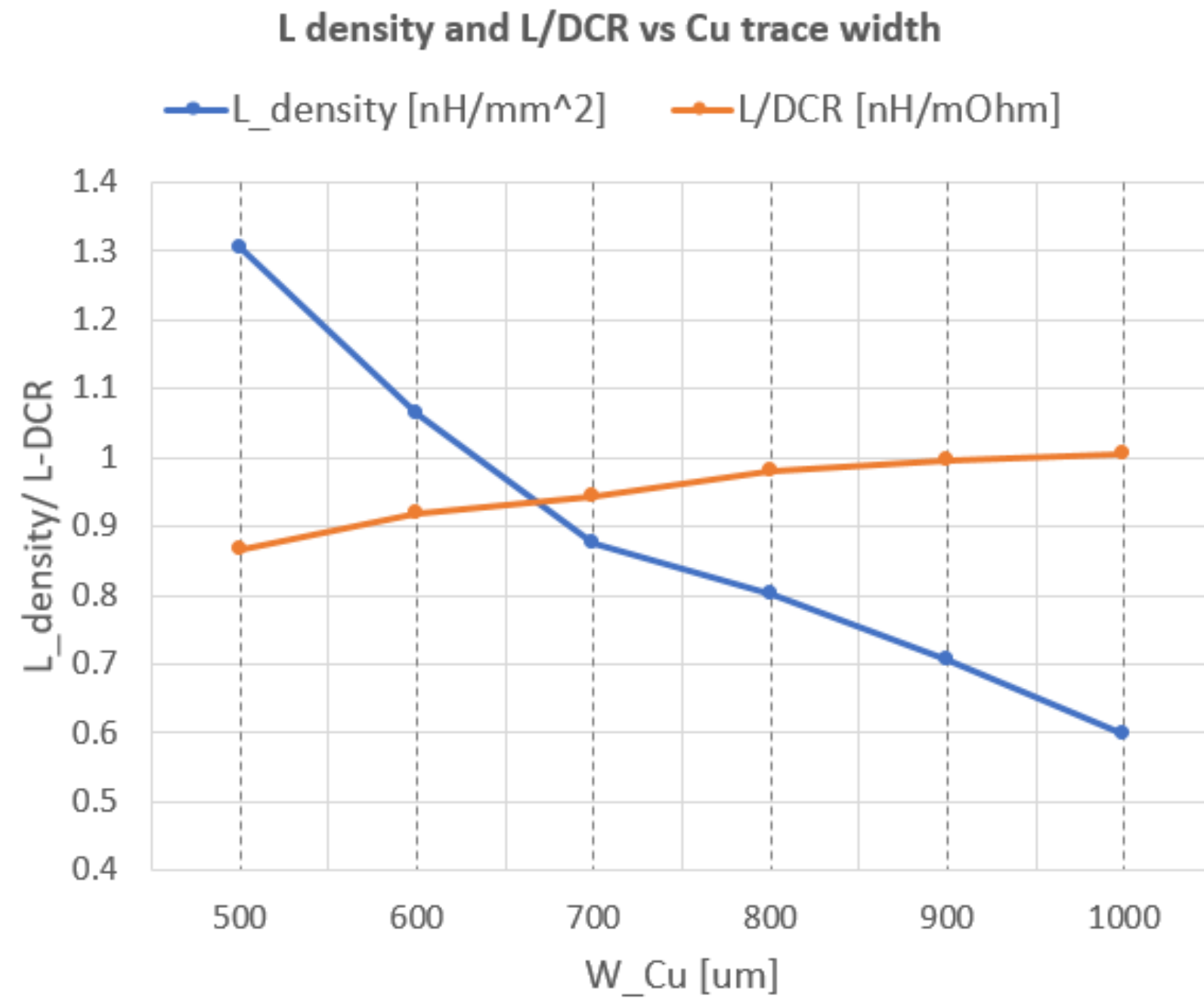
[11] H. K. Krishnamurthy et al., "A Digitally Controlled Fully Integrated Voltage Regulator With 3-D-TSV-Based On-Die Solenoid Inductor With a Planar Magnetic Core for 3-D-Stacked Die Applications in 14-nm Tri-Gate CMOS," in IEEE Journal of Solid-State Circuits, vol. 53, no. 4, pp. 1038-1048, April 2018, doi: 10.1109/JSSC.2017.2773637.

[12] “Fully Integrated Ultra Low Voltage Cold Start System for Thermal Energy Harvesting”, Preetinder Garcha, Master of Science in Electrical Engineering and Computer Science at the MASSACHUSETTS INSTITUTE OF TECHNOLOGY June 2016



## Background – A Design Space Exploration

# L-density and L/DCR vs Cu width and footprint



For increasing Cu trace width, Inductance density decreases (i.e. inductor footprint increases) at a faster rate than the increase in the L/DCR ratio.

